Title
HIJING: A Monte Carlo Model for Multiple Jet Production in pp, pA, and AA Collisions

Journal
Physical Review D, 44(11)

Authors
Wang, X.-N.
Gyulassy, M.

Publication Date
1991-07-01

LBL-31036
Preprint

Lawrence Berkeley Laboratory
UNIVERSITY OF CALIFORNIA

Submitted to Physical Review D

HIJING: A Monte Carlo Model for Multiple Jet Production in *pp*, *pA*, and *AA* Collisions

X.-N. Wang and M. Gyulassy

July 1991

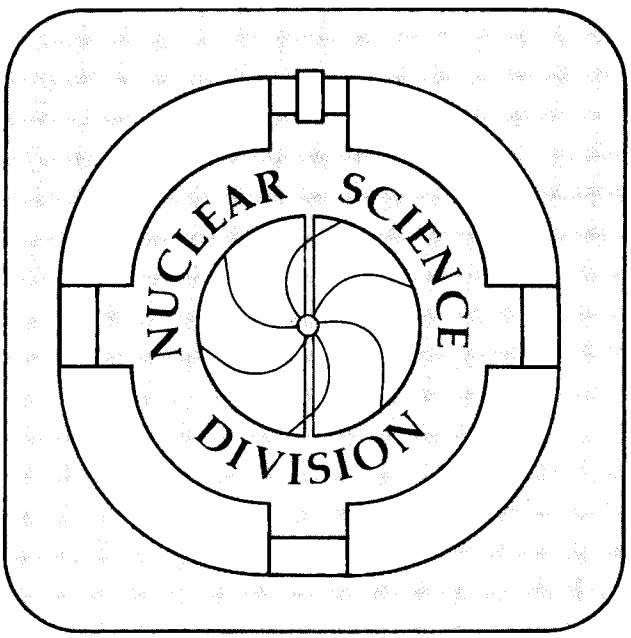

Prepared for the U.S. Department of Energy under Contract Number DE-AC03-76SF00098

DISCLAIMER

LBL-31036

HIJING: A Monte Carlo Model for Multiple Jet Production in pp, pA, and AA Collisions*

Xin-Nian Wang† and Miklos Gyulassy

Nuclear Science Division, Mailstop 70A-3307
Lawrence Berkeley Laboratory
University of California, Berkeley, CA 94720 USA

Abstract

Combining PQCD inspired models for multiple jet production with low p_T multi-string phenomenology, we develop a Monte Carlo event generator, HIJING, to study jet and multi-particle production in high energy pp, pA, and AA collisions. The model includes multiple mini-jet production, nuclear shadowing of parton distribution functions, and a schematic mechanism of jet interactions in dense matter. Glauber geometry for multiple collisions is used to calculate pA and AA collisions. The phenomenological parameters are adjusted to reproduce essential features of pp multi-particle production data for a wide energy range($\sqrt{s}$ = 5–2000 GeV). Illustrative tests of the model on $p+A$ and light ion $B+A$ data at $\sqrt{s} = 20$ GeV/n and predictions for $Au+Au$ at RHIC energies ($\sqrt{s} = 200$ GeV/n) are given.

PACS numbers: 13.87.Ce, 11.80.La, 13.85.Hd, 25.70.Np

---

*This work was supported by the Director, Office of Energy Research, Division of Nuclear Physics of the Office of High Energy and Nuclear Physics of the U.S. Department of Energy under Contract No. DE-AC03-76SF00098.

†Address after October 1, 1991: Department of Physics, Duke University, Durham, NC 27706, USA.

1 Introduction

One of the goals of experiments on nuclear collisions at ultra-relativistic energies $\sqrt{s} \gtrsim 200$ GeV/n is to study ultra-dense matter in the laboratory and to search for evidence of the predicted QCD phase transition to a quark-gluon plasma (QGP)[1]. However, in order to recognize new physics in the collision of heavy nuclei due to the formation of a QGP, methods need to be developed to subtract the background due to unrelated non-equilibrium processes. That background arises mainly from the convolution of multiple inelastic nucleon-nucleon processes in nuclear collisions. For example, QGP formation is not expected in pp or light ion induced reactions because the energy densities achieved and the reaction times and volumes are too small. Nevertheless, such reactions already lead to a wide variety of intricate and interesting correlations among the observables due to the interplay between non-perturbative low p_T physics, multiple mini-jet production, and the rare high p_T QCD processes.

Monte Carlo event generators are useful to perform such complex convolutions and to produce output that can be compared directly with a wide variety of experimental observables , *e.g.* limited acceptance calorimeters, charged particle correlations, *etc.* In addition, complete event generators are useful for planning and design of future experiments. Of course, many aspects of multi-particle production even in pp collisions remain uncertain at this time. Comparison of results produced by different event generators or by varying the model parameters are therefore needed to provide a measure of the extrapolation uncertainties to $A+A$ collisions. Finally, there is a need to develop event generators for $A+A$ collisions to serve as theoretical laboratories to test proposed signatures and probes of ultra-dense matter such as jet quenching[2].

In this paper we present a new Monte Carlo model, HIJING (Heavy Ion Jet INteraction Generator), to address a wide range of phenomenological problems involving nuclear collisions. The main features included in HIJING are as follows:

1. Soft beam jets are modelled by diquark-quark strings with gluon kinks along the lines of the Lund FRITIOF and Dual Parton Model (DPM)[3, 4]. In addition, multiple low p_T exchanges among the end point constituents are included to model initial state interactions.

2. Multiple mini-jet production with initial and final state radiation is included along the lines of the PYTHIA model[5]. In our treatment, an eikonal formalism is used to calculate the number of mini-jets per inelastic pp collision. For triggered high p_T processes, the associated enhancement of semi-hard and soft background is calculated self-consistently.

3. Exact diffuse nuclear geometry is used to calculate the impact parameter dependence of the number of inelastic processes[6].

4. An impact parameter dependent parton structure function is introduced to study the sensitivity of observables to nuclear shadowing, especially of the gluon structure functions.

5. A model for jet quenching is included to enable the study of the dependence of moderate and high p_T observables on an assumed energy loss dE/dx of partons traversing the produced dense matter.

The formulation of HIJING was guided by the Lund FRITIOF[3] and Dual Parton Model[4] phenomenology for soft $B + A$ reactions at intermediate energies $\sqrt{s} \lesssim 20$ GeV/n and the successful implementation of perturbative QCD (PQCD) processes in the PYTHIA model[5] for hadronic interactions. We note that many other models for AA collisions have been developed (e.g., ATTILA[6], VENUS[7], HIJET[8],RQMD[9] and MCMC[10]). However, HIJING is presently the only one incorporating the PQCD approach[5] of PYTHIA to multiple jet processes and the nuclear effects such as parton shadowing and jet quenching. This is especially emphasized in HIJING because semi-hard processes are expected to play a crucial role at Relativistic Heavy Ion Collider

(RHIC) ($\sqrt{s} \sim 200$ GeV/n) and Large Hadron Collider (LHC) ($\sqrt{s} \sim 6$ TeV/n) energies [11]-[14]. By incorporating the successful multi-string phenomenology for low p_T interactions at intermediate energies, HIJING also provides a link between the dominant non-perturbative fragmentation physics at intermediate SPS energies and the perturbative QCD physics at the highest collider energies presently foreseen. What HIJING does not incorporate is the mechanism for final state interactions among the low p_T produced particles. Therefore the approach to local equilibration cannot be addressed. HIJING is designed mainly to explore the range of possible initial conditions that may occur in nuclear collisions at collider energies. On the other hand, we have also included a schematic model of final state interactions of high p_T partons in terms of an effective energy loss parameter, dE/dx, to study the magnitude of jet quenching that may occur in such collisions.

Multiple mini-jets have been estimated[11, 13] to produce up to 50% (80%) of the transverse energy per unit rapidity in the collisions of heavy nuclei at RHIC (LHC) energies. Mini-jets involve calculable PQCD processes with transverse momentum scales $p_T \gtrsim 2$ GeV/c. While not resolvable as distinct jets, they are expected to lead to a wide variety of correlations among observables such as transverse momentum, strangeness, and fluctuation enhancements with increasing A that compete with expected signatures of a QGP. Therefore, it is especially important to calculate these background processes as reliably as possible. In addition, it has been shown that multiple mini-jet production is important in $p\bar{p}$ interactions to account for the increase of total cross section[15] with energy, the increase of average transverse momentum with charged multiplicity[17] and the violation of Koba-Nielsen-Olesen (KNO) scaling of the charged multiplicity distributions[5, 16].

The interactions of high p_T jets in the transient dense medium produced in high energy nuclear collisions is of interest as a diagnostic tool[2]. High p_T partons are produced on a very short time scale compared to the low p_T partons in the same collision.

Such jets provide an effective "external" probe of the matter since the initial rate and spectrum of hard processes is reliably calculable via PQCD [18]. Furthermore, fragmentation models[19, 20] now have the capability to reproduce many of the essential aspects of the hadronization of such jets. What jets probe in nuclear collisions is the stopping power, dE/dx, of dense matter for high energy quarks and gluons. That stopping power is in turn controlled by μ_D^2, where μ_D^{-1} is the color screening (Debye) scale in that medium. Estimates for dE/dx in a QGP indicate that dE/dx could be considerably different in a QGP than in ordinary hadronic or nuclear matter[2]. In particular a rapid variation of μ_D near the phase transition point could lead to a variation of jet quenching phenomenon that may serve as one of the signatures of the QGP transition. However, because of the large background expected due to mini-jets[11]-[14], the detection of a high p_T jets is also more difficult than in $p\bar{p}$ collisions. Only a full Monte Carlo study incorporating that large background can evaluate the feasibility and sensitivity of this observable.

In this paper, we discuss in detail the assumptions and formulation of the HIJING model and present some numerical results for pp, pA and AA collisions. The FORTRAN source code is available for distribution. The outline of this paper is as follows: Section 2 concentrates on those aspects of the model specific to hadron-hadron interactions while section 3 introduces our approach to multiple inelastic interactions in pA and AA collisions. In section 2.1, we review the the eikonal formalism for hadron interaction cross sections as discussed in Ref.[16]. We show how the probability of multiple mini-jet production in pp collisions depends not only on the cutoff scale p_0 but also on the impact parameter dependent partonic overlap function. A new feature of the formalism developed in section 2.2 is to show how those probabilities change when high p_T jets are triggered. In section 2.3 we discuss our implementation of the non-perturbative multi-string phenomenology for beam jets emphasizing similarities and differences with the Lund and DPM models. In section 2.4, we discuss our model

of initial state interactions to account for the higher $\langle p_T \rangle$ of produced particles in pp vs e^+e^- and the so called sea-gull effect. The implementation of mini-jets and hard jets with initial and final state radiations included in HIJING is discussed in section 2.5. In section 3.1, the nuclear geometry and binary collision approximations for pA and AA are discussed. In section 3.2 we introduce a model of the impact parameter dependent nuclear shadowing of parton structure functions. In section 3.3, the mechanism used to quench jets in terms of gluon splitting is discussed. Numerical results for $p + A$ and $O + A$ reactions at $E_{lab} = 200$ GeV/n are compared to data in section 3.4. Finally, we present predictions for $Au + Au$ at RHIC energies. Section 4 concludes with a summary and discussion of future applications of HIJING.

2 Nucleon-nucleon collisions

HIJING is based on a particular model of high energy pp inelastic collisions. In this section, the detailed assumptions and parameters together with the pp and $p\bar{p}$ data used to constrain that model are discussed.

2.1 Cross Sections for Multiple Jet Production

The cross section of hard parton scatterings in PQCD can be written as[22]

$$\frac{d\sigma_{jet}}{dp_T^2 dy_1 dy_2} = K \sum_{a,b} x_1 f_a(x_1, p_T^2) x_2 f_b(x_2, p_T^2) d\sigma^{ab}(\hat{s}, \hat{t}, \hat{u})/d\hat{t}, \qquad (1)$$

where the summation runs over all parton species, y_1 and y_2 are the rapidities of the scattered partons, and x_1 and x_2 are the light-cone momentum fractions carried by the initial partons. These variables are related by $x_1 = x_T(e^{y_1} + e^{y_2})/2$, $x_2 = x_T(e^{-y_1} + e^{-y_2})/2$, $x_T = 2p_T/\sqrt{s}$. The PQCD cross sections, $d\sigma_{ab}$, depend on the subprocess variables $\hat{s} = x_1 x_2 s$, $\hat{t} = -p_T^2(1+\exp(y_2 - y_1))$, and $\hat{u} = -p_T^2(1+\exp(y_1 - y_2))$. In HIJING the structure functions, $f_a(x, Q^2)$, are taken to be the Duke-Owens[21]

structure function set 1, as implemented in PYTHIA[5]. This parameterization for $f_a(x,Q^2)$ is adequate through RHIC energies. For higher energies the EHLQ parametrization[22] can be used. A factor, $K \approx 2$, is included to correct the lowest order PQCD rates for next to leading order effects.

The integrated inclusive jet cross section with $p_T > p_0$, is defined by

$$\sigma_{jet} = \int_{p_0^2}^{s/4} dp_T^2 dy_1 dy_2 \frac{1}{2} \frac{d\sigma_{jet}}{dp_T^2 dy_1 dy_2}. \tag{2}$$

Note that a jet in our terminology refers to a *pair* of high p_T partons from a hard scattering. The average number of jets with $p_T \geq p_0$ in pp collisions is thus $N_{jet}^{pp} = \sigma_{jet}/\sigma_{in}$. The integration region above is restricted to a region such that $x_1 < 1$,$x_2 < 1$ and $x_1 x_2 > 4p_T^2/s$. This leads for a fixed p_T to the restriction

$$\begin{aligned} -\ln(2/x_T - e^{-y_1}) \leq y_2 \leq \ln(2/x_T - e^{y_1}), \\ \mid y_1 \mid \leq \ln(1/x_T + \sqrt{1/x_T^2 - 1}). \end{aligned} \tag{3}$$

Though the cross sections for three or four partons production can be estimated perturbatively[23], we take a probabilistic approach[16, 24] to multiple mini-jet production. To calculate the probability of multiple mini-jets at a scale $p_0 \sim 2$ GeV/c, our main dynamical assumption is that they are independent. This holds as long as their average number is not too large. Given an interaction transverse area, $\sim \pi/p_0^2$, for processes with $p_T \sim p_0$, independence requires that the total interaction area is less than πR_N^2, where $R_N \approx 0.85$ fm is the nucleon radius, i.e.,

$$\sigma_{jet} \lesssim (p_0 R_N)^2 \sigma_{in} \equiv \sigma_{max} \ . \tag{4}$$

For $p_0 \gtrsim 2$ GeV/c, and $\sigma_{in} \approx 40$ mb, the right hand side is $\sigma_{max} \approx 3$ barns, and thus

the independent approximation should hold up to the highest energies foreseen. For nuclear collisions the total number of jets is given by

$$N_{jet}^{AA} = T_{AA}(b)\sigma_{jet} \ , \tag{5}$$

where $T_{AA}(b)$ is the nuclear overlap function[11] at an impact parameter b. For $b = 0$, $T_{AA} \approx A^2/\pi R_A^2$, and multiple mini-jets may be independent as long as

$$\sigma_{jet} \lesssim (p_0 R_A)^2 \pi R_A^2/A^2 \approx 2\sigma_{max}/A^{2/3} \ . \tag{6}$$

For $A = 197$ the right hand side is 180 mb, and thus independence should apply up to LHC energies (see Fig. 1 below). On the other hand, nuclear shadowing of the initial structure functions cannot be neglected when the longitudinal wavelength $1/p_L$ of the parton exceeds the Lorentz contracted nuclear diameter, $2R_A/\gamma$. We will return to this point in section 3.2.

Given the independent jet approximation, the probability for multiple mini-jet production is given by[16, 24]

$$g_j(b) = \frac{[\sigma_{jet}T_N(b)]^j}{j!} e^{-\sigma_{jet}T_N(b)}, \ \ j \geq 1. \tag{7}$$

where $T_N(b)$ is partonic overlap function between the two nucleons at impact parameter b, and $\sigma_{jet}T_N(b)$ is the corresponding average number of mini-jets.

On the other hand the probability of no mini-jet production depends on a non-perturbative inclusive cross section, σ_{soft}, for soft processes defined via

$$g_0(b) = [1 - e^{-\sigma_{soft}T_N(b)}]e^{-\sigma_{jet}T_N(b)}. \tag{8}$$

The total inelastic cross section of the nucleon-nucleon collisions is then

$$\sigma_{in} = \int d^2b \sum_{j=0}^{\infty} g_j(b) = \int d^2b[1 - e^{-(\sigma_{soft}+\sigma_{jet})T_N(b)}]. \tag{9}$$

In the eikonal formalism, the elastic, inelastic and total cross sections are related by

$$\sigma_{el} = \pi \int_0^{\infty} db^2 \left[1 - e^{-\chi(b,s)}\right]^2, \tag{10}$$

$$\sigma_{in} = \pi \int_0^{\infty} db^2 \left[1 - e^{-2\chi(b,s)}\right], \tag{11}$$

$$\sigma_{tot} = 2\pi \int_0^{\infty} db^2 \left[1 - e^{-\chi(b,s)}\right], \tag{12}$$

in the limit that the real part of the scattering amplitude can be neglected and thus that the eikonal function $\chi(b,s)$ is real. Comparing Eq. 11 with Eq. 9 one can relate $\chi(b,s)$ to

$$\begin{aligned} \chi(b,s) &\equiv \chi_s(b,s) + \chi_h(b,s), \\ &= \frac{1}{2}\sigma_{soft}(s)T_N(b,s) + \frac{1}{2}\sigma_{jet}(s)T_N(b,s). \end{aligned} \tag{13}$$

As in Ref. [16], we assume that the energy dependent partonic overlap function can be approximated by the Fourier transform of a dipole form factor as

$$T_N(b,s) = \frac{\chi_0(\xi)}{\sigma_{soft}(s)}, \tag{14}$$

with

$$\chi_0(\xi) = \frac{\mu_0^2}{48}(\mu_0\xi)^3 K_3(\mu_0\xi), \quad \xi = b/b_0(s), \tag{15}$$

where $\mu_0 = 3.9$ and $\pi b_0^2(s) \equiv \sigma_{soft}(s)/2$ providing a measure of the geometrical size

of the nucleon. With this assumption, the eikonal function can be written as,

$$\chi(b,s) \equiv \chi(\xi,s) = \chi_0(\xi)[1 + \sigma_{jet}(s)/\sigma_{soft}(s)] \; . \tag{16}$$

This form insures that geometrical scaling[25, 26] is recovered at low energies when $\sigma_{jet} \ll \sigma_{soft}$. Integrating Eqs. 7 and 8 over the impact parameter and dividing by σ_{in}, the normalized probabilities for no and $j \geq 1$ number of jet productions with $p_T > p_0$ in an inelastic event are given by,

$$G_0 = \frac{\pi}{\sigma_{in}} \int_0^\infty db^2 [1 - e^{-2\chi_s(b,s)}] e^{-2\chi_h(b,s)}, \tag{17}$$

$$G_j = \frac{\pi}{\sigma_{in}} \int_0^\infty db^2 \frac{[2\chi_h(b,s)]^j}{j!} e^{-2\chi_h(b,s)}. \tag{18}$$

Choosing $p_0 \simeq 2$ GeV/c and assuming a constant value of $\sigma_{soft} = 57$ mb at high energies, the calculated cross sections and the multiplicity distribution in $p\bar{p}$ collisions agree well with experiments[16]. This is then the model we use to simulate multiple jets production at the level of nucleon-nucleon collisions in HIJING Monte Carlo program. In Fig. 1, the calculated total cross sections of pp or $p\bar{p}$ collisions are shown as a function of $\sqrt{s}$ (solid line) together with experimental data[26]-[31]. The dashed line corresponds to the total inclusive jet cross section. In Fig. 2 the probability distributions of multiple jet production G_j is shown for two different energies. The distribution becomes broader at higher energies showing the increasing importance of multiple mini-jet production.

Once the number of jets is determined, PYTHIA subroutines[5] are used to generate the kinetic variables of the scattered partons. In Fig. 3 we show that the calculated inclusive jet cross section as a function of the transverse momentum p_T agrees well with the UA1 data[32]. We note that the calculated histograms reflect only the distributions of the scattered partons and no attempt was made in this comparison to

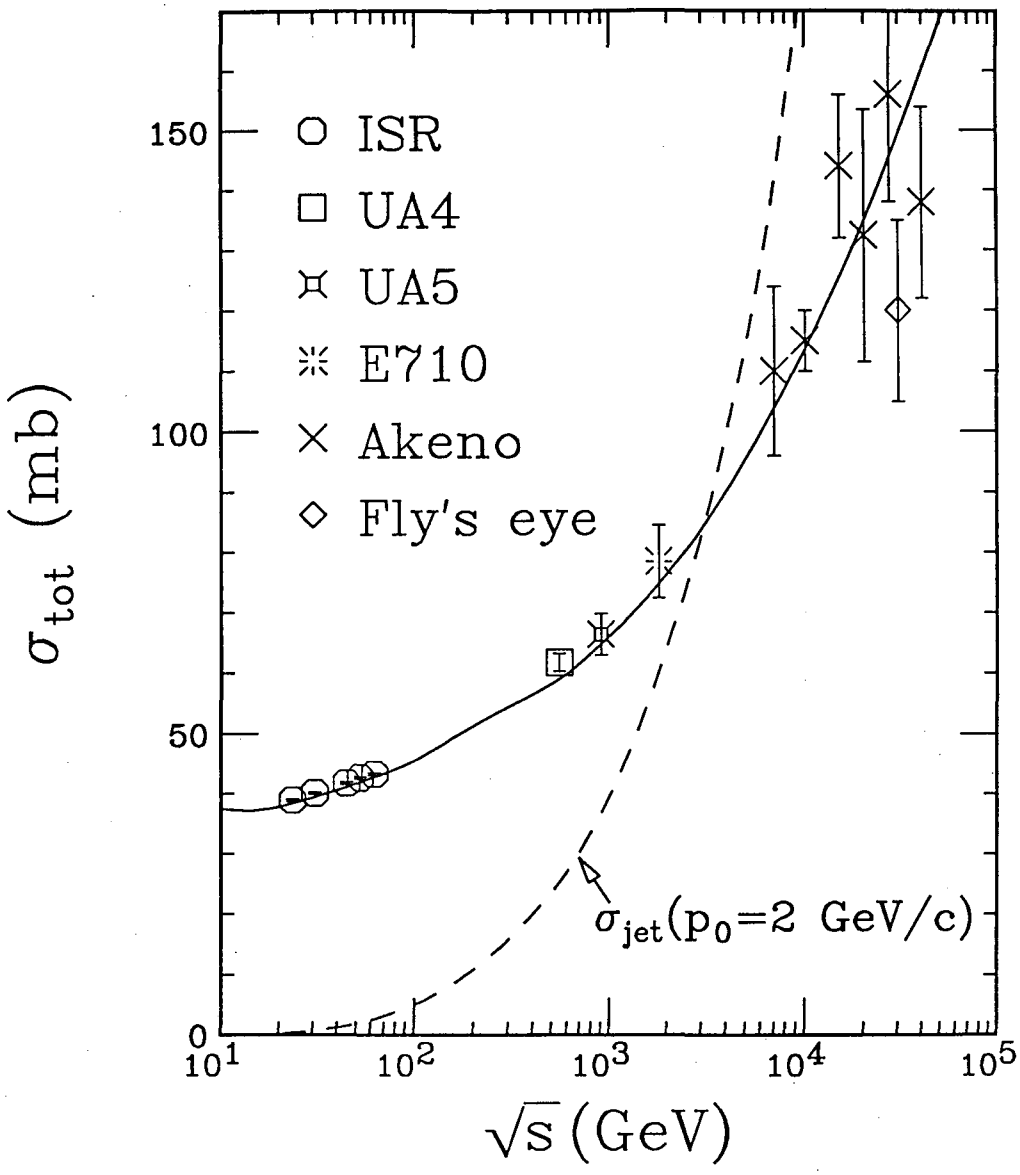

Fig. 1 The total pp and $p\bar{p}$ cross sections as a function of $\sqrt{s}$. The solid line is from HIJING calculation and data are from Refs. [26]-[31]. The dashed line is the inclusive jet cross section with p_0 =2 GeV/c.

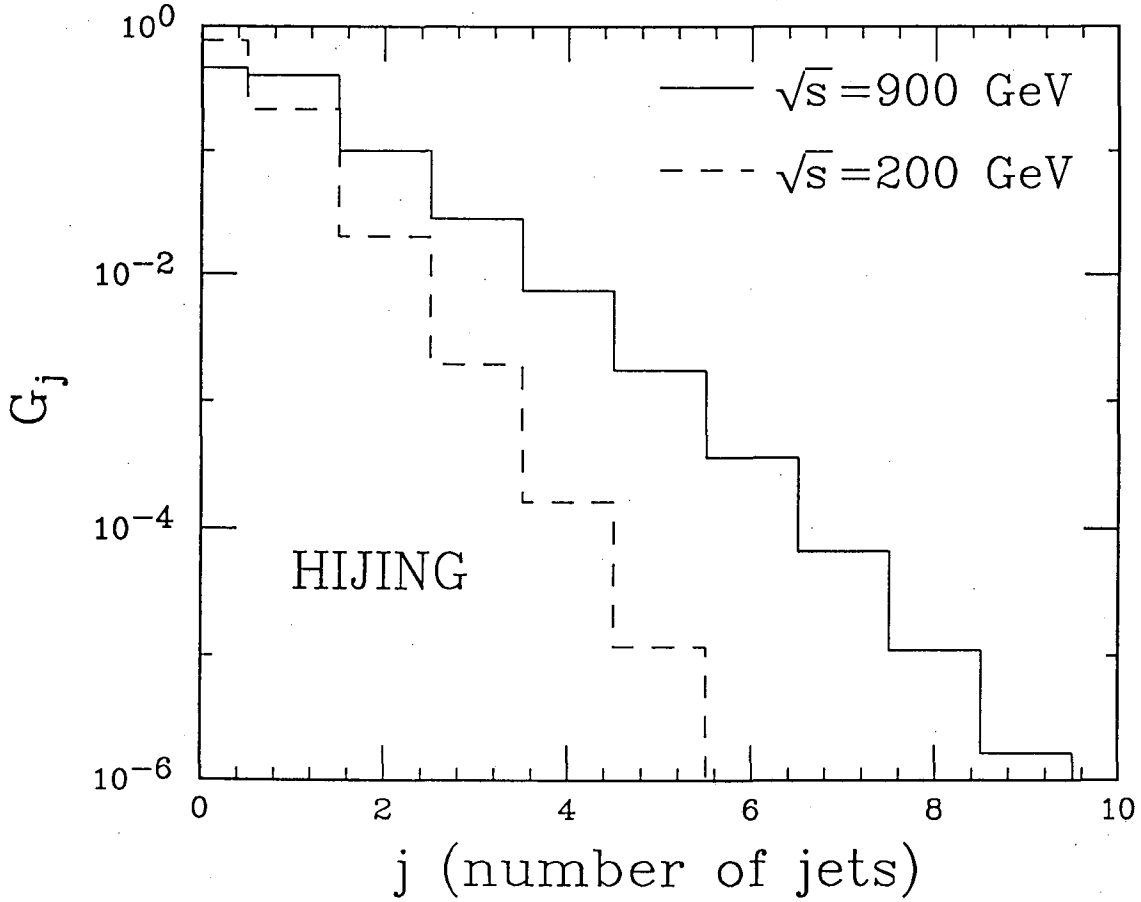

Fig. 2 HIJING calculation of the probability distribution G_j for j number of mini-jets at $\sqrt{s}$ = 200 (dashed histogram) and 900 GeV (solid histogram).

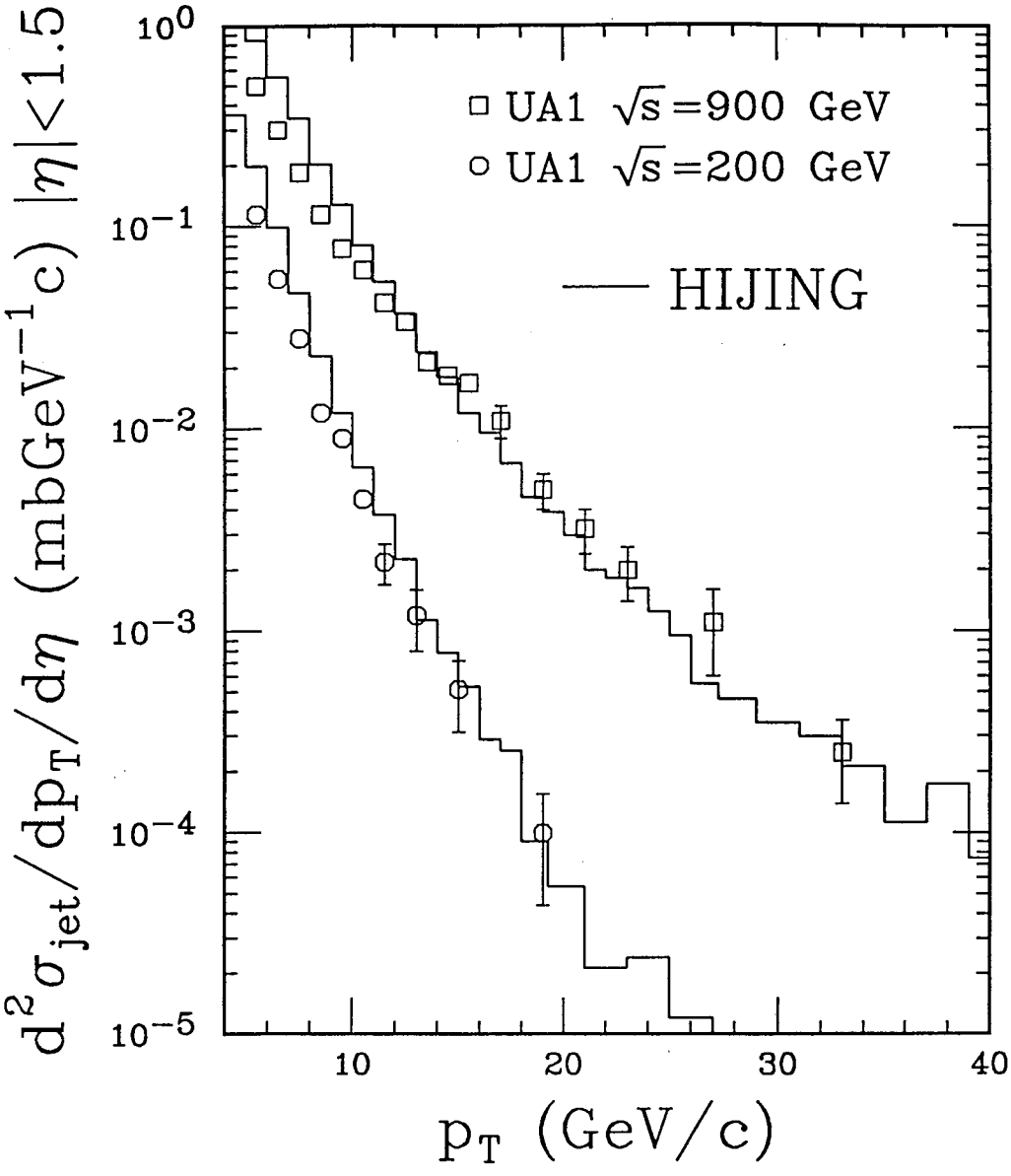

Fig. 3 The inclusive jet cross section at $\eta = 0$ as a function of p_T at two different collider energies. The UA1 data are from Ref. [32]. The histograms are for the simulated partons in HIJING from hard scatterings before final state radiation.

simulate the calorimetric definition of jets in UA1 (see Sec. 2.5 for more quantitative comparison with high p_T hadron spectra).

We regard the mini-jet scale p_0 as a model dependent phenomenological parameter separating the PQCD dynamics at high p_T from the non-perturbative low p_T regime. The value $p_0 = 2$ GeV/c was chosen by fitting the high energy total cross sections assuming that the cross section for soft processes is independent of energy[16]. We regard σ_{soft} as a measure of the geometrical size of the hadron to account for geometrical scaling at low energies[25, 26]. It is important for the overall consistency of the model that p_0 turns out to be sufficiently large[11, 15] that PQCD can be reasonably applied for $p_T \geq p_0$.

2.2 Triggering on jet production

Because the differential cross section of jet production changes several orders in magnitude from small to large p_T, there is often a need to trigger on a jet with a specified p_T cut in order to increase the efficiency of simulations. This trigger can however change the probability of multiple mini-jet production and thus the whole event structure[5]. In particular, such rare processes will tend to occur most often when the impact parameter is small so as to increase the partonic overlap. However, at small impact parameters production of multiple jets is also enhanced. In order to understand this dynamical triggering effect, we look more closely at the probability distribution in Eq. 7.

The jet cross section in the interval Δp_T at p_T is

$$\Delta\sigma_{jet}(p_T) = \frac{d\sigma_{jet}}{dp_T}\Delta p_T. \tag{19}$$

According to the assumption of independent jet production, the probability distribu-

tion of j such jets is,

$$g_j(b, p_T) = \frac{[\Delta\sigma_{jet}(p_T)T_N(b)]^j}{j!} e^{-\Delta\sigma_{jet}(p_T)T_N(b)}. \tag{20}$$

Of course this can only hold for p_T far from the kinematical limit. By convoluting all the distributions $g_j(b, p_T)$ with $p_T \geq p_0$, we recover Eq. 7.

Now we can divide jets into two groups, one having $p_T > p_T^{trig}$ and another one having $p_0 < p_T < p_T^{trig}$. According to this grouping, Eq. 7 can be rewritten as

$$\begin{aligned} g_j(b) &= \sum_{j_0=0}^{\infty}\sum_{j_t=0}^{\infty} \frac{[(\sigma_{jet}(p_0) - \sigma_{jet}(p_T^{trig}))T_N(b)]^{j_0}}{j_0!} e^{-[\sigma_{jet}(p_0)-\sigma_{jet}(p_T^{trig})]T_N(b)} \\ &\quad \frac{[\sigma_{jet}(p_T^{trig})T_N(b)]^{j_t}}{j_t!} e^{-\sigma_{jet}(p_T^{trig})T_N(b)}\delta_{j,j_0+j_t}. \end{aligned} \tag{21}$$

If we want to trigger on events which have at least one jet with p_T above p_T^{trig}, we have to sum over j_t beginning at $j_t = 1$. Therefore, the probability for the triggered events is

$$g_j^{trig}(b) = \frac{[\sigma_{jet}(p_0)T_N(b)]^j}{j!} \left\{1 - \left[\frac{\sigma_{jet}(p_0) - \sigma_{jet}(p_T^{trig})}{\sigma_{jet}(p_0)}\right]^j\right\} e^{-\sigma_{jet}(p_0)T_N(b)}. \tag{22}$$

Obviously $g_j^{trig}(b)$ reduces to $g_j(b)$ when $p_T^{trig} = p_0$. Summing over $j \geq 1$ leads to expected total probability for having at least one jet with $p_T > p_T^{trig}$:

$$g^{trig}(b) = 1 - e^{-\sigma_{jet}(p_T^{trig})T_N(b)}. \tag{23}$$

Since $g_j^{trig}(b)$ differs from $g_j(b)$, the triggering of a particular jet therefore changes the production rates of the other jets in the same event. This triggering effect is especially significant when we consider large p_T^{trig}. Because $\sigma_{jet}(p_T^{trig}) \ll \sigma_{jet}(p_0)$, we

can approximate the cross section of the triggered events by

$$\sigma^{trig} = \int d^2b[1 - e^{-\sigma_{jet}(p_T^{trig})T_N(b)}] \approx \sigma_{jet}(p_T^{trig}). \tag{24}$$

By expanding Eq. 22 in the power of $\sigma_{jet}(p_T^{trig})$ we have the conditional probability

$$\begin{aligned} G_j^{trig} &\equiv \frac{1}{\sigma^{trig}} \int d^2b\, g_j^{trig}(b) \\ &\approx \frac{1}{\sigma_{jet}(p_0)} \int d^2b \frac{[\sigma_{jet}(p_0)T_N(b)]^j}{j!} j e^{-\sigma_{jet}(p_0)T_N(b)}, \\ &= \frac{\sigma_{in}}{\sigma_{jet}(p_0)} j G_j. \end{aligned} \tag{25}$$

It is clear from the above equation that it becomes more probable to produce multiple jets due to the triggering on a high p_T jet and the increase from ordinary distribution is proportional to the number of jet, j.

We implement Eq. 22 in HIJING by simulating two Poisson-like multiple jets distributions with inclusive cross sections $\sigma_{jet}(p_0) - \sigma_{jet}(p_T^{trig})$ and $\sigma_{jet}(p_T^{trig})$ respectively. We demand that the second one must have at least one jet and convolute the two together. To demonstrate this triggering effect we plot in Fig. 4 the ratio between the probability distributions of multiple jets production with and without triggering at $\sqrt{s} = 900$ GeV for two different p_T^{trig}. Here all the distributions are normalized to 1 for $j \geq 1$. We see that there is continuous increase of the enhancement of multiple jets production in the triggered distributions. Especially for $p_T^{trig} \geq 10$ GeV/c (solid line), the enhancement is almost linear to the number of jet productions j. This enhancement of multiple jet production in high p_T processes can lead to a number of interesting consequences for the event structure in pp and $p\bar{p}$ which will be discussed in a separate publication.

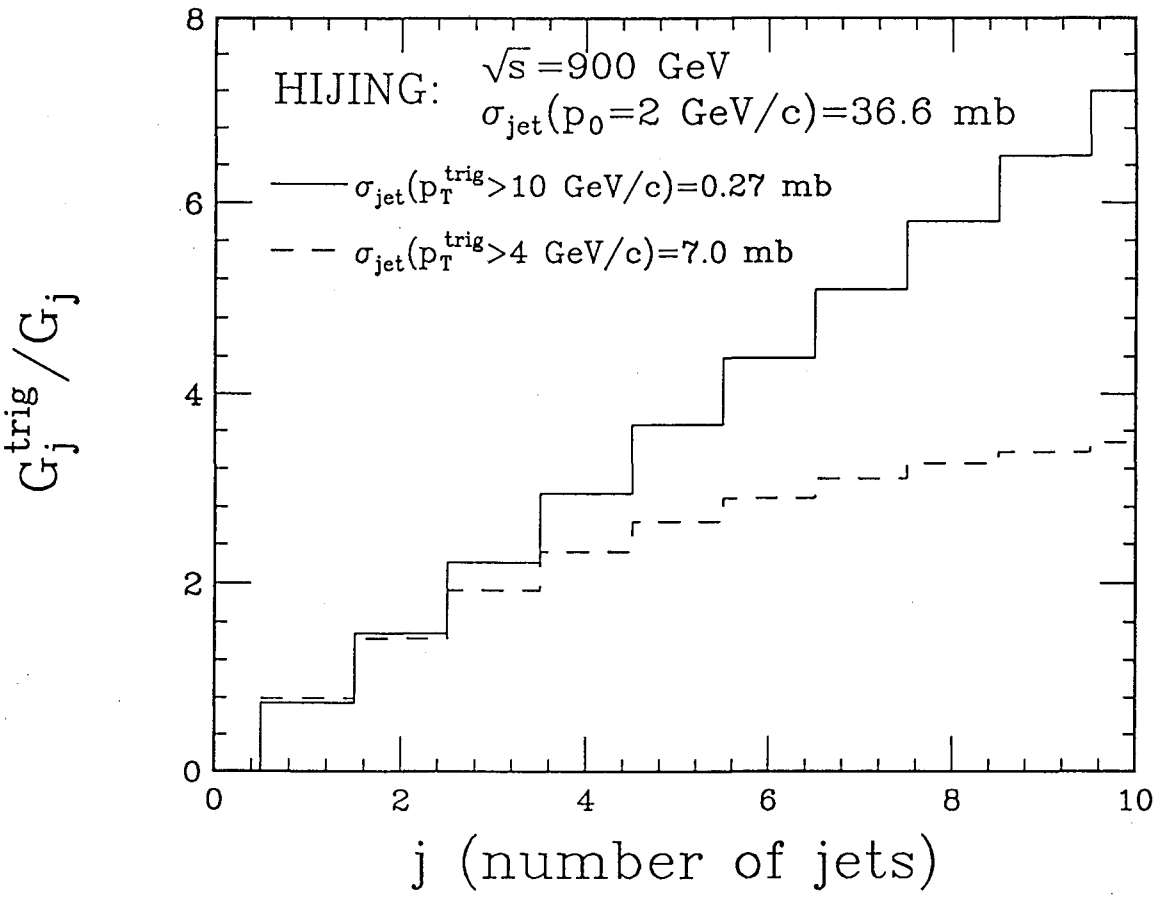

Fig. 4 HIJING calculation of the ratio G_j^{trig}/G_j between the probability distribution of j number of mini-jets with and without triggering at $\sqrt{s} = 900$ GeV. The untriggered jets have a p_T cutoff of $p_0 = 2$ GeV/c while the triggered jet has $p_T^{trig} \geq 4$ (dashed histogram) and 10 GeV/c (solid histogram).

2.3 Soft interactions

From Fig. 1 we see that the dominant mechanism of multi-particle production for $\sqrt{s} \lesssim 100$ GeV is soft interactions. In HIJING we adopt a variant of the multiple string phenomenology developed in Refs. [3]-[7] as a model for such interactions. The picture behind that phenomenology is that multiple soft gluon exchanges between the constituent quarks or diquarks in hadrons can lead to longitudinal string-like excitations of those hadrons. Those interactions must naturally involve small p_T kicks to the constituent quarks as well as induced soft gluon radiation that can be modelled by introducing kinks in the strings. The strings are assumed to decay independently via quark-antiquark creation using, in our case, the Lund JETSET7.2[33] fragmentation routine to describe the hadronization.

The string excitation is achieved by a collective momentum transfer $P = (P^+, P^-, \mathbf{p}_T)$ between the hadrons. Given initial light-cone momenta

$$p_1 = (p_1^+, \frac{m_1^2}{p_1^+}, \mathbf{0}_T), \quad p_2 = (\frac{m_2^2}{p_2^-}, p_2^-, \mathbf{0}_T), \tag{26}$$

with $(p_1^+ + m_2^2/p_2^-)(p_2^- + m_1^2/p_1^+) \equiv s$, the final momenta of the strings are assumed to be

$$p_1' = (p_1^+ - P^+, \frac{m_1^2}{p_1^+} + P^-, \mathbf{p}_T), \quad p_2' = (\frac{m_2^2}{p_2^-} + P^+, p_2^- - P^-, -\mathbf{p}_T). \tag{27}$$

The remarkable feature of soft interactions is that low transverse momentum exchange processes with $p_T \lesssim 1$ GeV/c can result in large effective light-cone momentum exchanges[3], giving rise to two excited hadrons or strings with large invariant mass. Defining

$$P^+ = x_+\sqrt{s} - \frac{m_2^2}{p_2^-}, \quad P^- = x_-\sqrt{s} - \frac{m_1^2}{p_1^+}, \tag{28}$$

the excited masses of the two strings will be

$$M_1^2 = x_-(1-x_+)s - p_T^2, \quad M_2^2 = x_+(1-x_-)s - p_T^2, \tag{29}$$

respectively. In HIJING, we require that the excited string mass must exceed a minimum value $M_{cut} = 1.5$ GeV, and therefore the kinematically allowed region of $x^{\pm}$ is restricted to

$$x_-(1-x_+) \geq M_{Tcut1}^2/s, \quad x_+(1-x_-) \geq M_{Tcut2}^2/s, \tag{30}$$

where $M_{Tcut1}^2 = M_{cut}^2 + p_T^2$, $M_{Tcut2}^2 = M_{cut}^2 + p_T^2$. Only collisions with

$$s \geq s_{min} = (M_{Tcut1} + M_{Tcut2})^2. \tag{31}$$

are allowed to form excited strings. Eq. 31 also determines the maximum p_T that the strings can obtain from the soft interactions. In events with both hard and soft processes, two strings are still assumed to form but with a kinetic boundary reduced by the hard scatterings.

In the FRITIOF model[3], the probability for light-cone momentum exchange is assumed to be $P(x_{\pm}) = 1/x_{\pm}$. This form is motivated by the idea that string formation results from elastic scattering of wee partons in the colliding hadrons. Indeed this assumption reproduces well the dM/M distribution observed in single diffractive events[34]. Therefore for single diffractive events which occur with the cross section determined empirically in Ref. [34] we take

$$P(x_{\pm}) = \frac{1}{(x_{\pm}^2 + c^2/s)^{1/2}}, \tag{32}$$

where $c = 0.1$ GeV.

In the FRITIOF scheme, this same excitation law is assumed to hold for non-single-diffractive events and in subsequent string-string interactions in pA and AA as well. For $\sqrt{s} \lesssim 100$ GeV, this assumption is consistent with data. However, at higher collider energies we find that this simple scheme overpredicts the width of the rapidity distribution for produced particles. We therefore chose instead an excitation probability more along the lines of the DPM model[4]

$$P(x_\pm) = \frac{(1.0 - x_\pm)^{1.5}}{(x_\pm^2 + c^2/s)^{1/4}}, \tag{33}$$

for nucleons and

$$P(x_\pm) = \frac{1}{(x_\pm^2 + c^2/s)^{1/4}[(1 - x_\pm)^2 + c^2/s]^{1/4}}, \tag{34}$$

for mesons. These distributions are motivated by Regge phenomenology and the idea that the leading strings involve color exchange between constituent valence quarks.

With the above ansatz, the rapidity distributions are in good agreement with the collider data (see Fig. 11 below). However, the fluctuations in multiplicity then turn out to be too small. This problem is solved in DPM by introducing multiple (sea $q\bar{q}$) strings. But, enhanced fluctuations can also be modelled by introducing induced gluon bremsstrahlung radiation in the form of kinks in the strings as proposed in the FRITIOF scheme. Because the latter model is easier to implement numerically, we use the FRITIOF radiation scheme to enhance the multiplicity fluctuations. Thus after determining the masses using Eqs. 33, 34, we utilize the subroutine AR3JET and ARORIE of FRITIOF1.7[3] to determine the rapidity and p_T of the kinks. However, since HIJING treats explicitly the mini-jet physics via PQCD, we limit the transverse momentum of kinks due to soft processes to below the mini-jet scale $p_0 = 2$

GeV/c. This limitation on soft radiation is a characteristic feature of induced gluon bremsstralung due to soft exchanges[35]. Thus, unlike FRITIOF which extends the soft radiation phenomenology to high p_T, HIJING restricts that phenomenology to $p_T < p_0$ and uses PQCD in the $p_T > p_0$ region.

We emphasize that the low p_T algorithm used in HIJING is a phenomenological model needed to incorporate non-perturbative aspects of beam jet physics. Many variants of soft dynamics can be envisioned, but none can be rigorously defended from fundamental QCD. One of the attractive aspects of going to the highest possible collider energies is that the theoretical uncertainties due to soft dynamics is reduced as more and more of the dynamics becomes dominated by calculable semi-hard and hard QCD processes.

In Fig. 5 , we show that our low p_T algorithm reproduces the energy dependence of multi-particle production at moderate energies [36, 37]. In Fig. 6, we show that the calculated multiplicity fluctuations are also in reasonable agreement with data at ISR energies[39]. In particular, KNO scaling is approximately reproduced at these energies.

In Fig. 7, we compare the data on proton rapidity distribution at $E_{lab} = 24$ GeV to HIJING. The distribution is less well reproduced than the data on meson production in Fig. 5. This could stem from using the default diquark fragmentation scheme of JETSET7.2. A better agreement with the baryon distribution data can be achieved by introducing additional diffractive mechanisms involving sea quark-antiquark chains as in DPM models[4, 7]. In the present version of HIJING, those mechanisms are not implemented.

2.4 Low p_T transfer

In addition to the low $p_T < p_0$ gluon kinks, HIJING includes an extra low $p_T < p_0$ transfer to the constituent quarks and diquarks at the string end points in soft

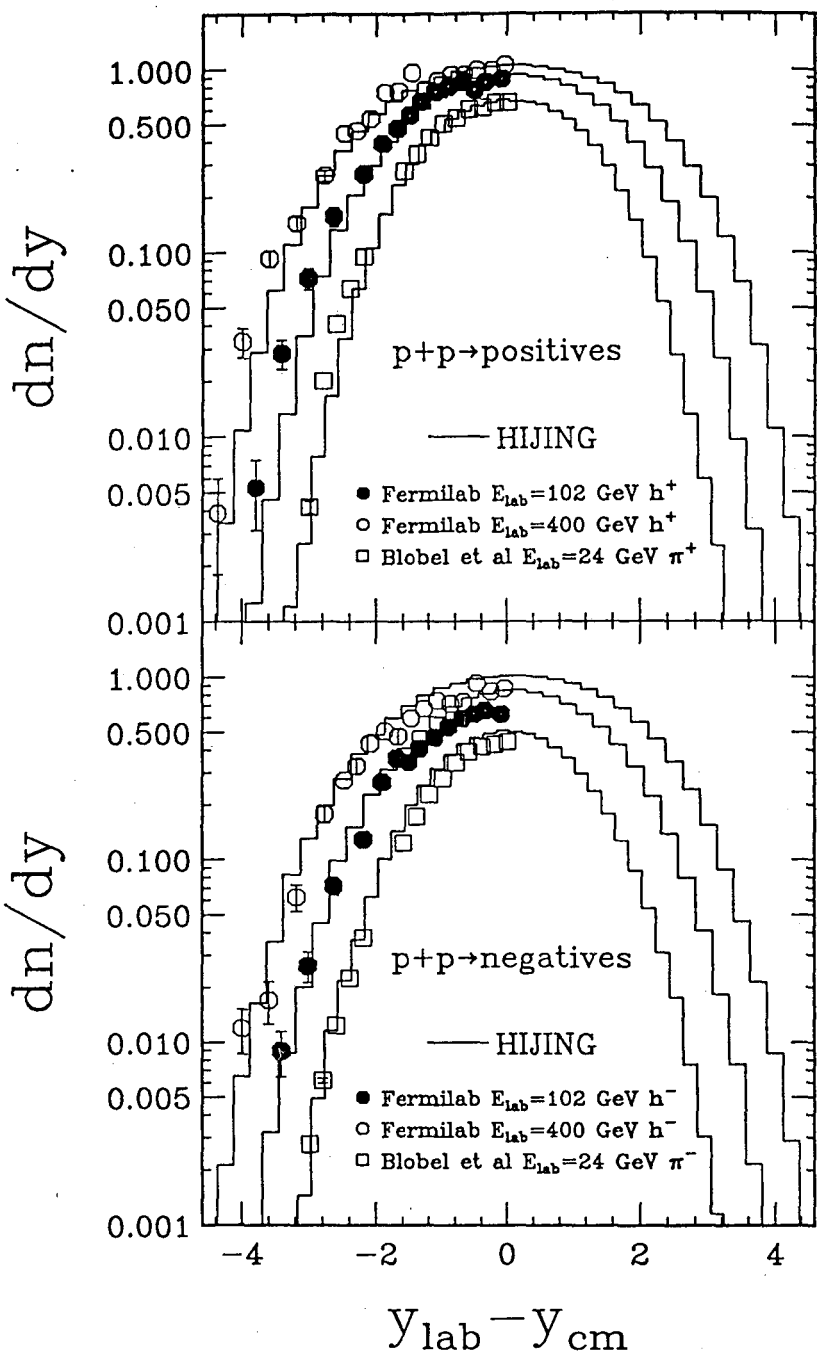

Fig. 5 The rapidity distributions of charged particles in pp collisions at three different energies. The data are from Refs. [36, 37] and the corresponding histograms are from HIJING calculation. The positive hadrons in both the calculation and data at E_{lab} =102 and 400 GeV do not include protons.

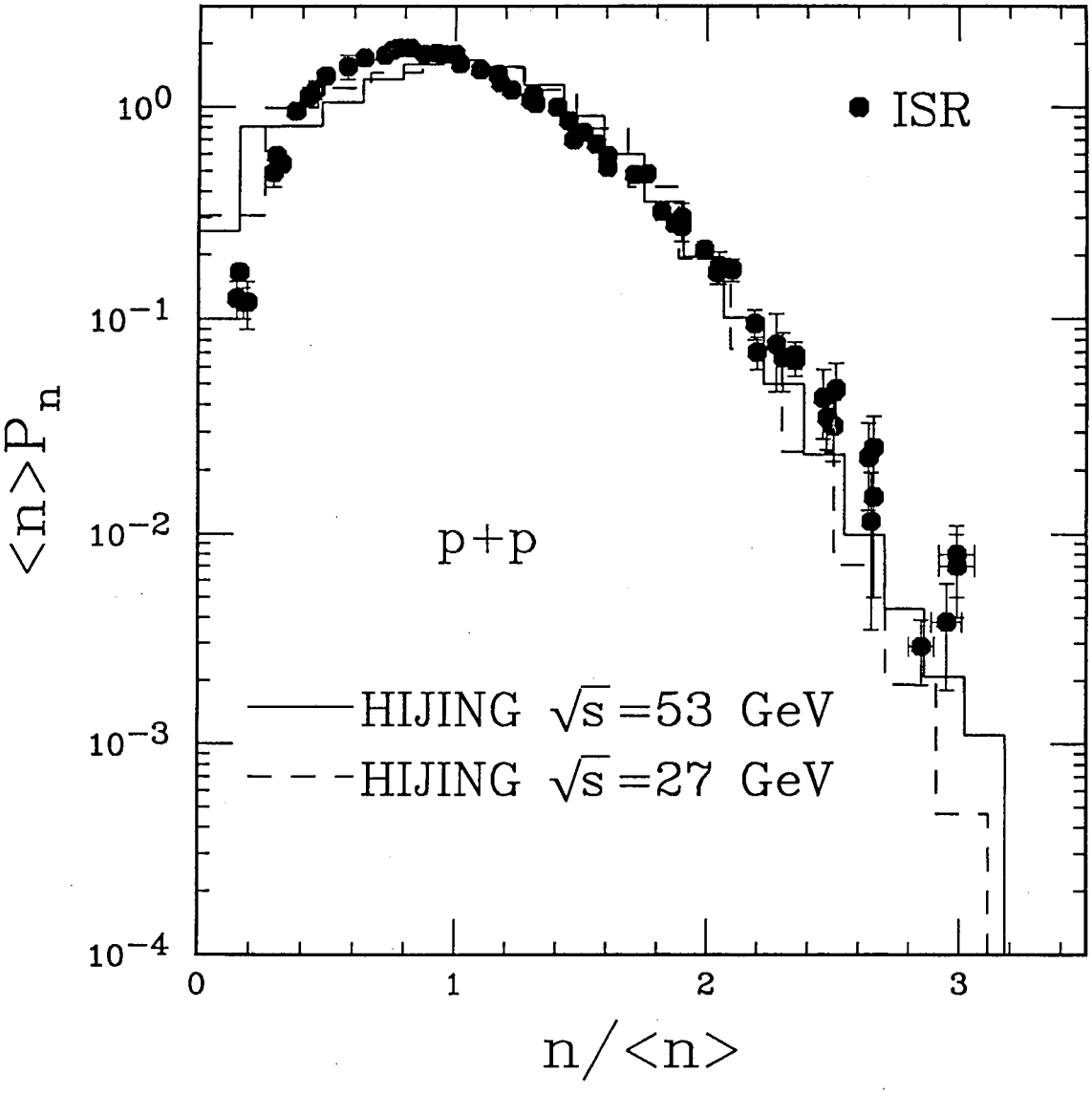

Fig. 6 The KNO plot of the charged multiplicity distributions in pp collisions. The ISR data are from Ref. [39]. The histograms are from HIJING calculation at $\sqrt{s} = 53$ (solid) and 27 GeV (dashed).

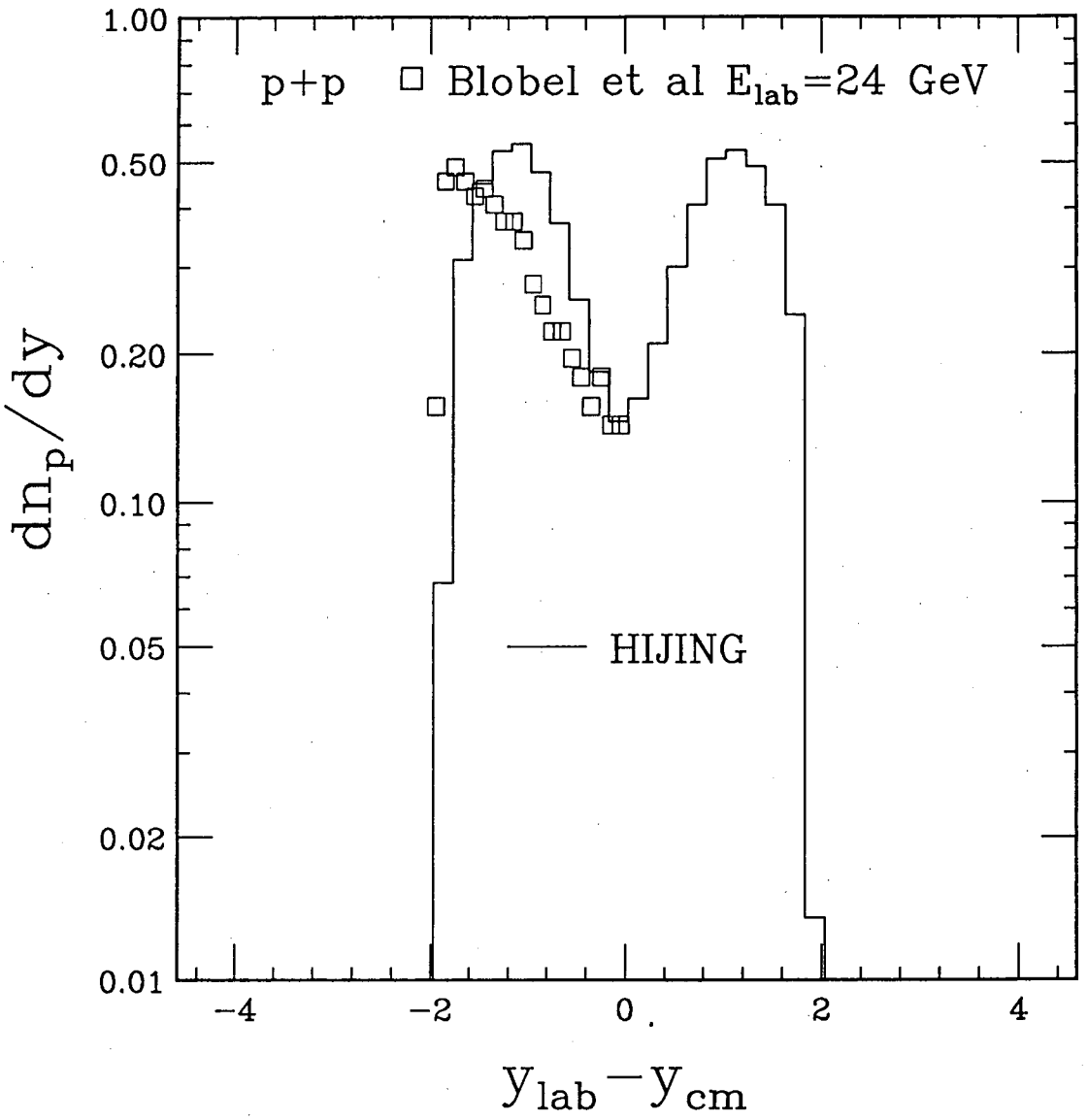

Fig. 7 The rapidity distribution of protons in pp collisions at $E_{lab} = 24$ GeV. The data are from Ref. [36] and histogram is HIJING result.

interactions. This effect is important at low energies $E_{lab} \sim 20$ GeV to account for the high p_T tails of the pion and proton distributions. We parameterize this transverse momentum kick probability by the following form

$$f_{kick}(p_T) \propto \theta(p_0 - p_T) \left[(p_T^2 + c^2)(p_T^2 + p_0^2)\right]^{-1}, \tag{35}$$

where as in Eq. 32 $c = 0.1$ GeV. This form was chosen to ensure that $f_{kick}(p_T)$ extrapolates smoothly to the regime of hard scatterings while varying more slowly for $p_T \ll p_0$. Since diquarks are composites, we assume that the p_T transfer to a diquark is further suppressed by a dipole form factor with a scale of 1 GeV/c.

This p_T kick to the quarks or diquarks during the soft interactions provides an increase in transverse momentum of produced hadrons. With the above choice for the soft transverse momentum distribution the p_T spectra of produced particle at low energies[36] are well reproduced by the model (solid histogram) as shown in Fig. 8. Note that HIJING uses the default settings of Lund Monte Carlo program JETSET 7.2. At these low energies, soft gluon radiation has a negligible effect. Without that extra soft p_T kick (dashed histogram), the transverse momentum from pair production in string fragmentation is not enough to account for the higher tail of the data at large p_T.

In Fig. 9, the averaged transverse momentum $\langle p_T \rangle$ is shown as a function of rapidity y_{lab} for negative charged particles. Both HIJING and experimental data[37] show a scaling behavior in the fragmentation region and a slight increase of $\langle p_T \rangle$ with energy in the central region. An alternate way to plot the same data is shown in Fig. 10. There $\langle p_T \rangle$ is plotted as a function of Feynman variable $x_f = 2\sqrt{p_T^2 + m^2}\sinh(y_{lab} - y_{cm})/\sqrt{s}$. Because x_f varies with $\sqrt{s}$ for fixed p_T and y_{lab}, the scaling of $\langle p_T \rangle$ in y_{lab} naturally leads to the energy dependence of the so-called sea-gull effect, which is mainly of kinematic origin.

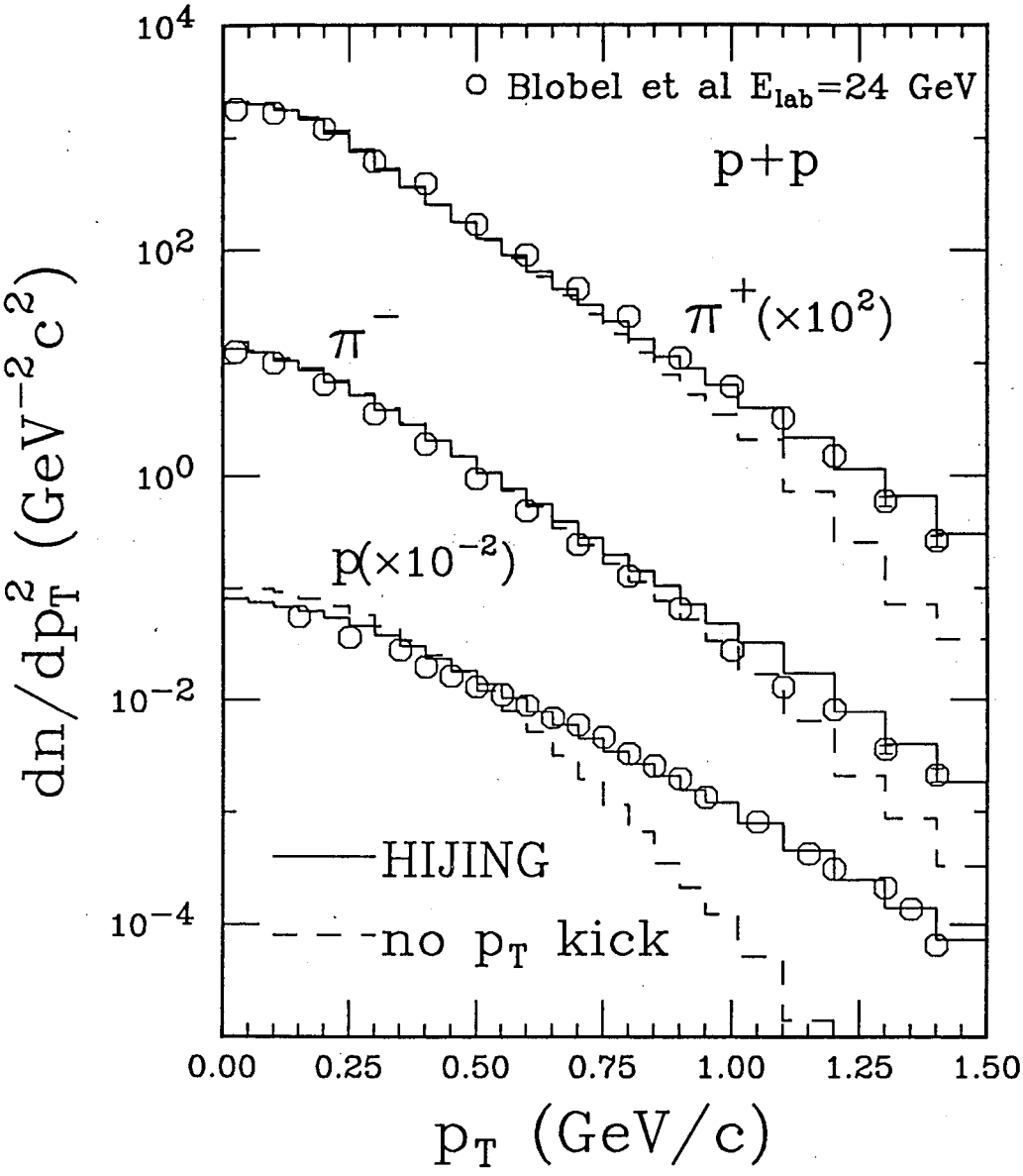

Fig. 8 The p_T distributions of charged particles in pp collisions at E_{lab} = 24 GeV. The data are from Ref. [36] and the histograms are from HIJING calculation with (solid) and without (dashed) soft p_T kick.

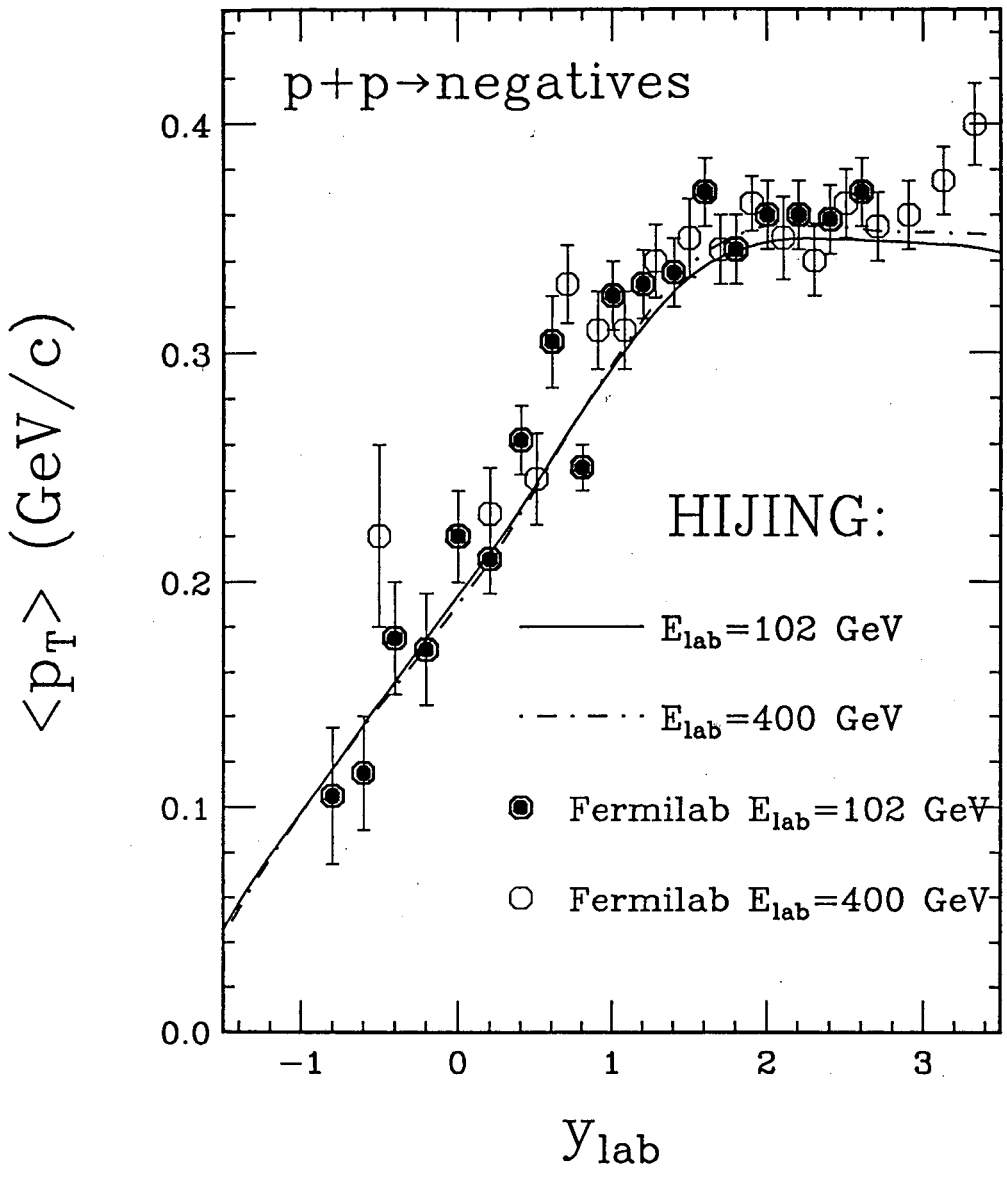

Fig. 9 $<p_T>$ as a function of y_{lab} for negative particles in pp collisions at E_{lab} = 102, 400 GeV. The data are from Ref. [37] and lines are from HIJING calculation.

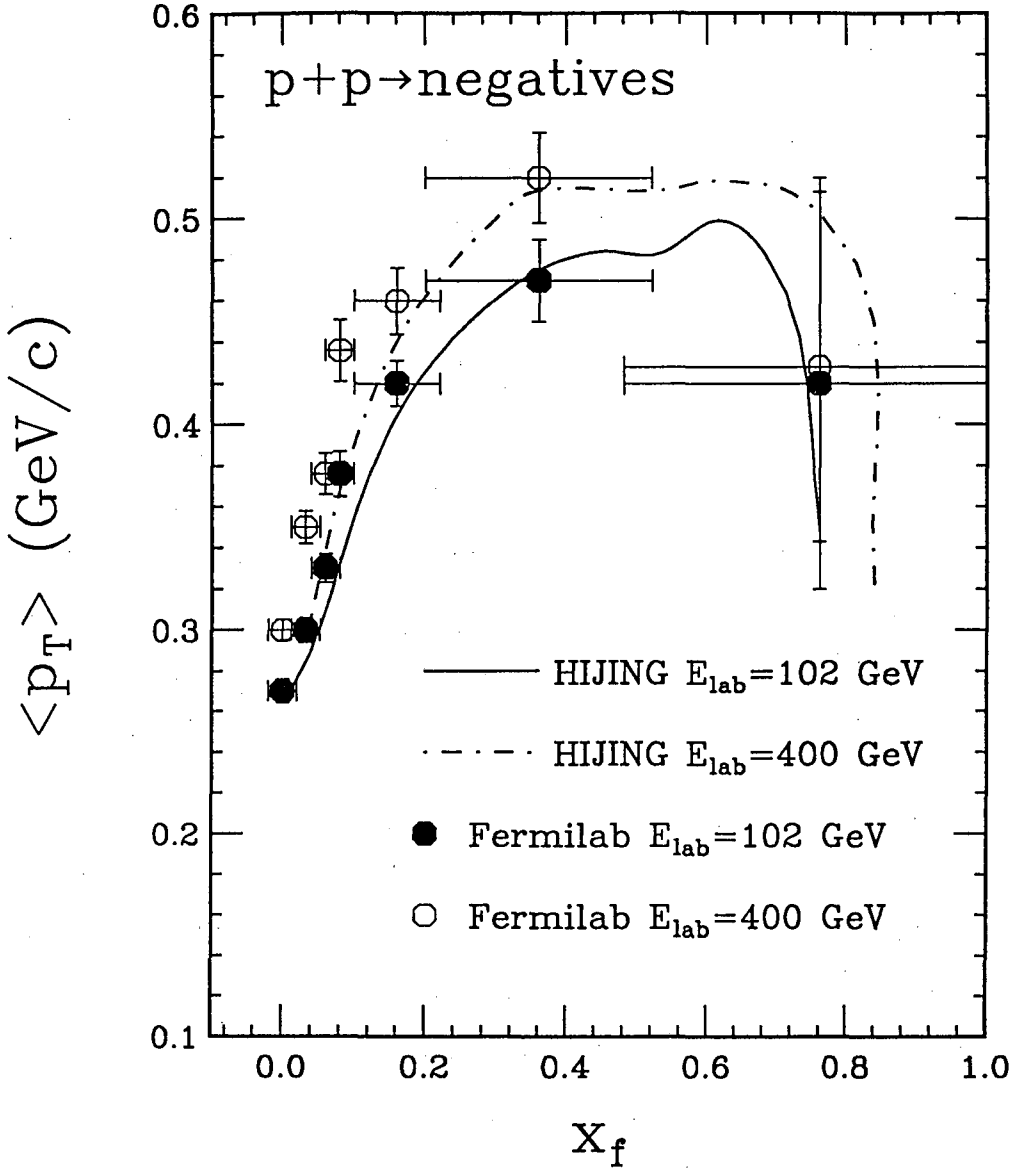

Fig. 10 $< p_T >$ as a function of $x_f \equiv 2m_T \sinh(y_{lab} - y_{cm})/\sqrt{s}$ for negative particles in pp collisions at $E_{lab} = 102$, 400 GeV. The data are from Ref. [37] and lines are from HIJING calculation.

2.5 Structure of multiple jet production

In inelastic pp interactions, at least two excited strings are produced. The color flow along the string is from one end-point to the other. Complications arise when one considers the color configuration of events with multiple hard interactions. Even though the color flow can be given by a consistent scheme[40] to a certain approximation in an event with one hard scattering, the color arrangement in multiple jets events can be very complex. This problem cannot be answered rigorously in PQCD as it deals with the long range correlations imposed on the multi-parton final state by confinement. For many inclusive observables, however, the final results fortunately do not appear to be sensitive to such effects[5]. For example in multi-gluon events, the end point partons can be connected in many different ways to the gluons. However, we have checked that the inclusive particle distributions are insensitive to that ordering. In HIJING all gluons are ordered simply according to their rapidities. This effectively minimizes the invariant mass of the string[5]. We also utilize that insensitivity to simplify the numerical treatment of hard processes involving one or more quarks or antiquarks. For rare events which have a hard process involving quarks or anti-quarks we restrict the subsequent ones to gluon-gluon scatterings. For numerical simplicity, the flavor of the final scattered quark or antiquark is, however, replaced by one of the valence quarks to fix the color flow. This prescription leads to a small error for flavor correlations but retains the correct rate and kinematics of those PQCD processes. We have checked in particular that the moderate high p_T K/π ratio is not sensitive to this simplification because gluon jets dominate in such observables.

Once the interaction cross sections and the number of jets produced at given impact parameter are determined as in Section 2.1, we use the PYTHIA Monte Carlo program to determine their kinetic variables, including the initial and final state radiations associated with each hard scattering. The accompanying soft interactions are treated as discussed above but with the energies of the scattered partons subtracted

from the total. The final hadronization stage is treated by the JETSET7.2 model.

In Fig. 11, we show the calculated and experimental results[41] on pseudo-rapidity distributions of charged particles in non-single-diffractive events of pp at $\sqrt{s} = 53$ GeV and $p\bar{p}$ collisions at $\sqrt{s} = 200$ GeV. HIJING (solid histograms) reproduces both the overall widening of the distribution and the increase of central density with the colliding energy. As a comparison, we also show the same calculated distributions when jet production is switched off (dashed lines). We note that mini-jet production is virtually negligible at ISR energies. At CERN Collider energy, however, mini-jets production becomes an important source of particle production in the central region. Without jets, the central density $dn_{ch}/d\eta(\eta = 0)$ is essentially independent of energy. The rise of the central density with energy due to jet production leads to a nonlinear increase of the total multiplicity as a function of $\ln(s)$[16].

The most convincing demonstration of the importance of jet production is seen in the p_T distribution of produced particles. Shown in Fig. 12, are the invariant inclusive cross sections as a function of p_T at the same two energies from HIJING (histograms) compared to the same collider data[42, 43]. Instead of being nearly an exponential function of p_T at low energies as shown in Fig. 8, the p_T distribution exhibits a power-law tail characteristic of PQCD. The successful reproduction of the magnitude and the energy dependence of the moderate high p_T tails is an important test for the overall consistency of this approach of combining soft string phenomenology with hard QCD dynamics.

The importance of multiple mini-jet production is also reflected in the multiplicity distributions and the underlying event structure. Plotted in Fig. 13 is the charged multiplicity distribution at $\sqrt{s} = 200$ GeV. The histograms are from HIJING calculation and the data points are from Ref. [44]. Also shown in the figure are the contributions to the multiplicity distribution from events with no jet production (dot-dashed histogram), one jet production (dashed histogram) and two or more

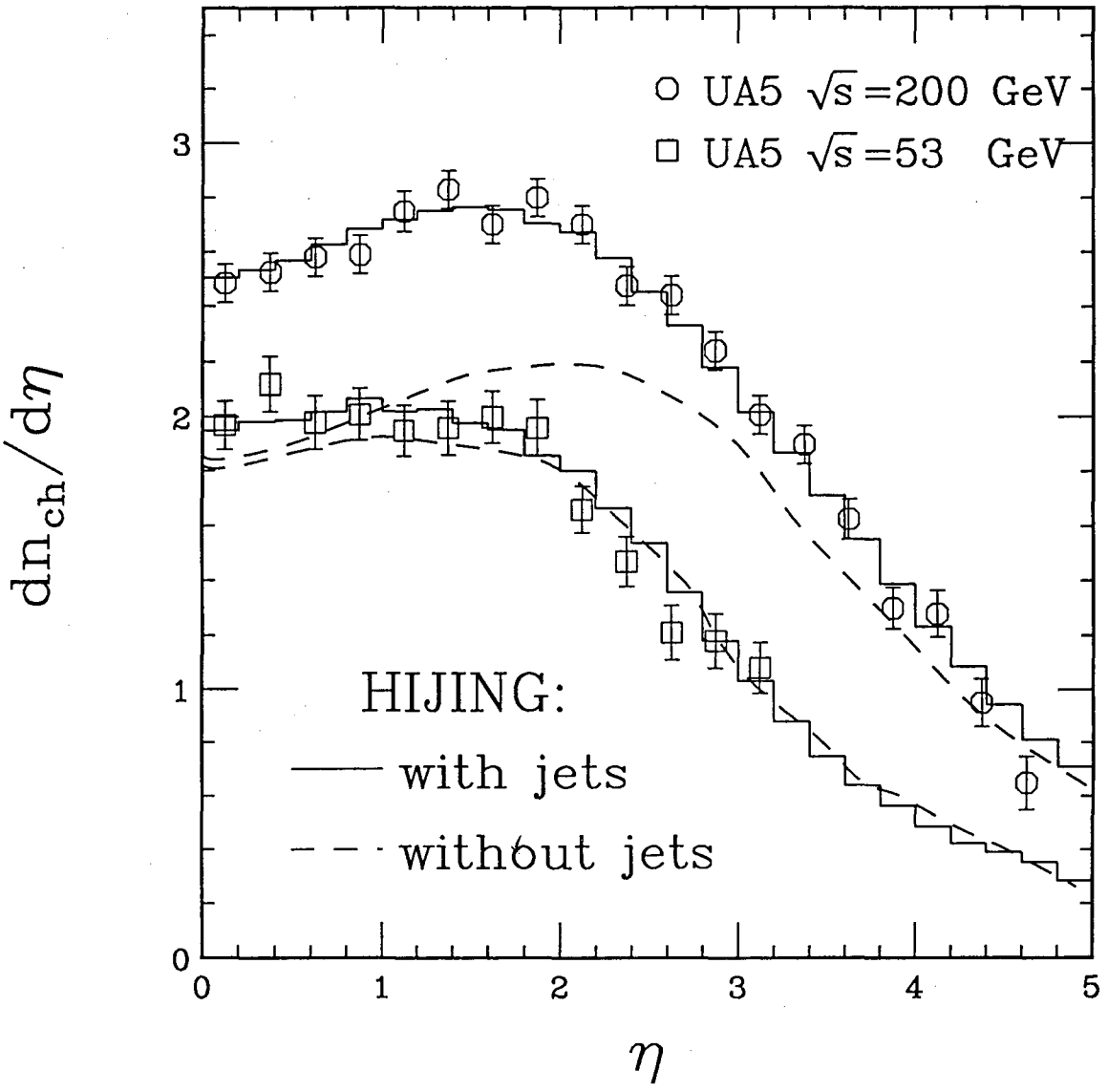

Fig. 11 Pseudo-rapidity distributions for charged particles in non-single-diffractive pp at $\sqrt{s} = 53$ GeV and $p\bar{p}$ collisions at $\sqrt{s} = 200$ GeV. The data are from Ref. [41] and the histograms are from HIJING calculation with (solid) and without (dashed lines) jet production.

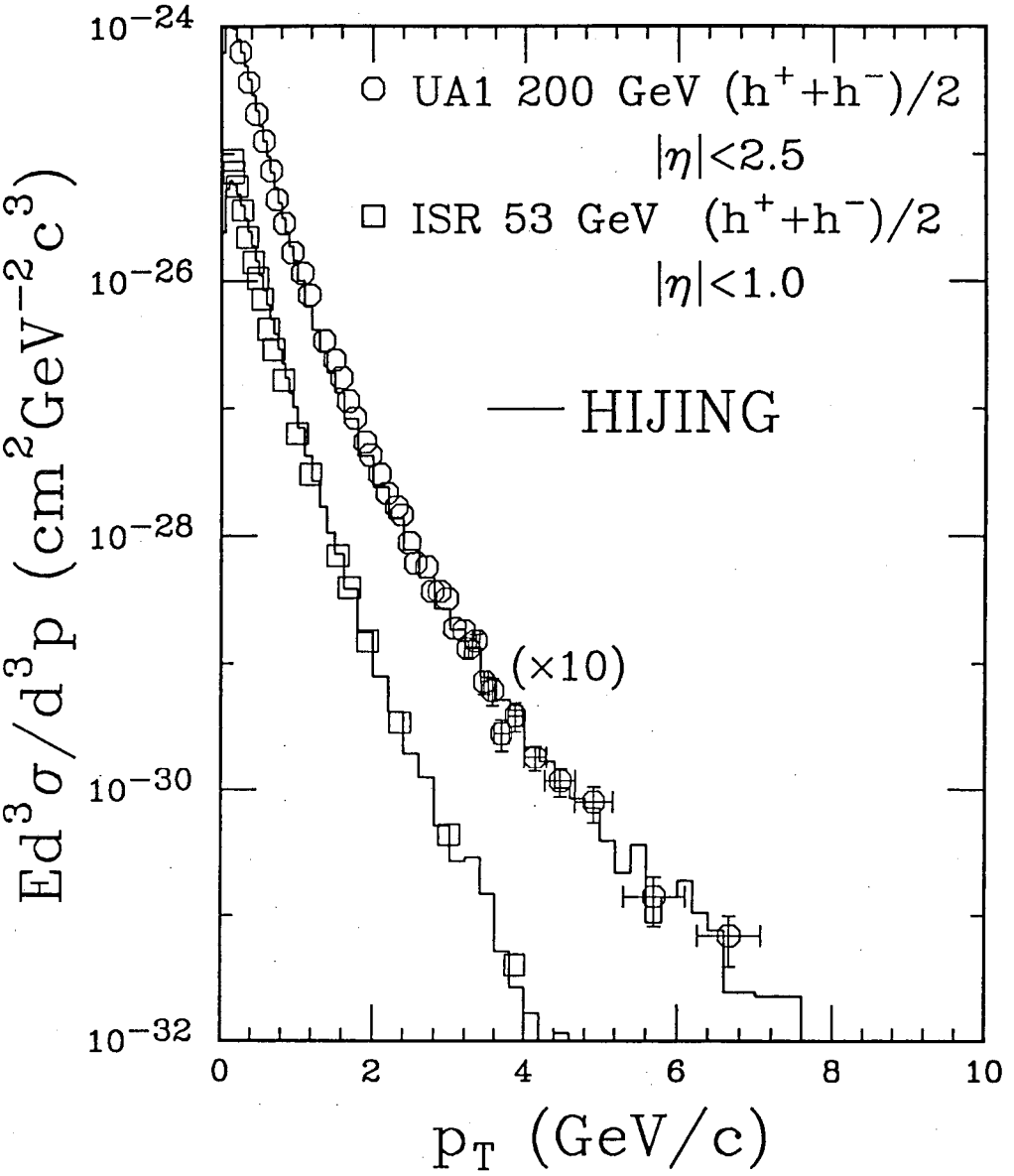

Fig. 12 Inclusive cross sections for charged hadrons as a function of p_T in pp at $\sqrt{s} = 53$ GeV and $p\bar{p}$ collisions at $\sqrt{s} = 200$ GeV. The data are from Refs. [42, 43] and histograms are from HIJING calculation.

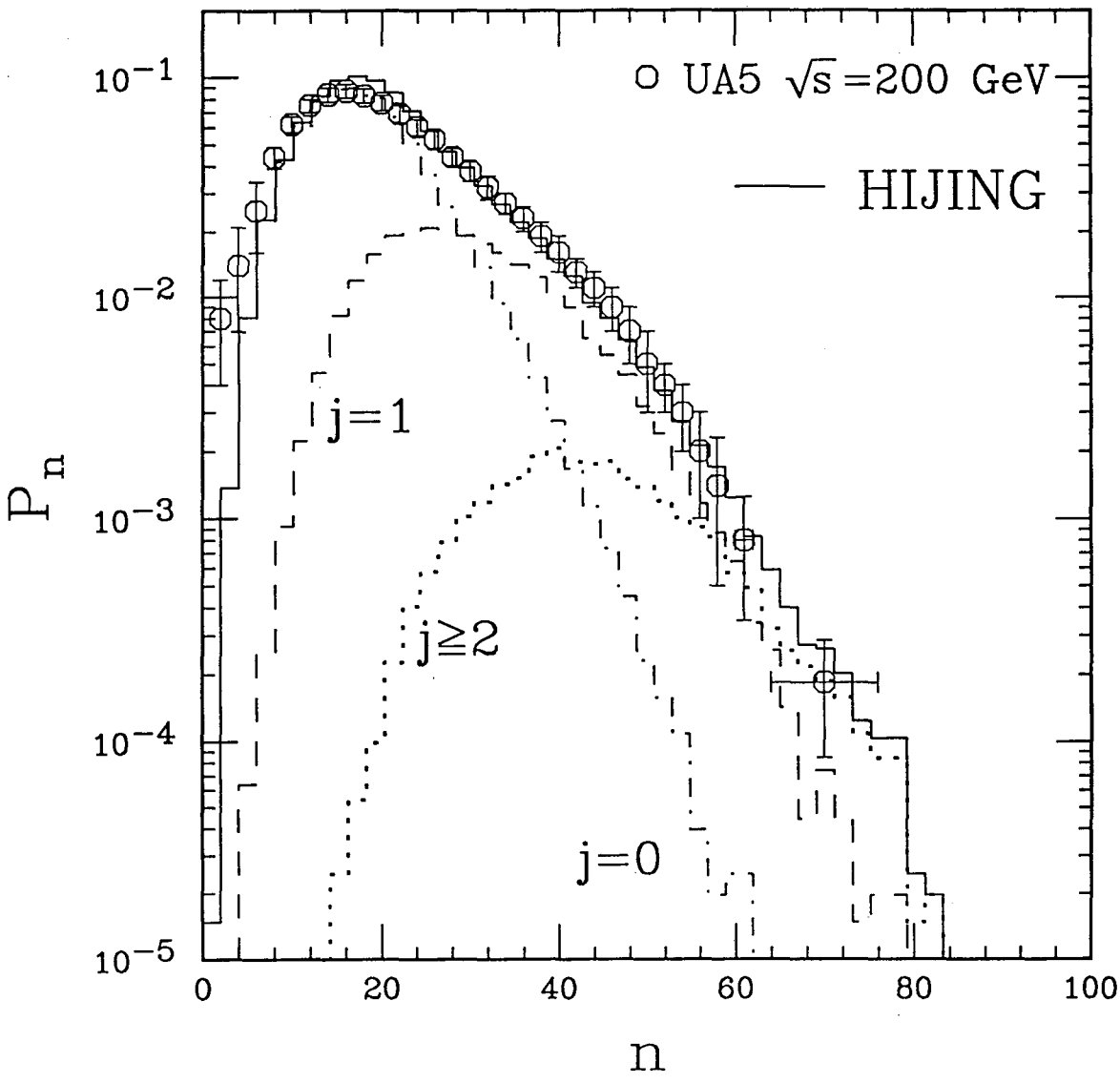

Fig. 13 Charged multiplicity distribution in $p\bar{p}$ collisions at $\sqrt{s} = 200$ GeV. The data are from Ref. [44]. The solid histogram is from HIJING calculation with contributions from events with $j = 0$ (dot-dashed histogram), $j = 1$ (dashed histogram) and $j \geq 2$ (dotted histogram) number of jet productions.

jet productions (dotted histogram). We can see that the low multiplicity events are dominated by those of no jet production while high multiplicity events are dominated by those of at least one jet production. The contributions from events of multiple jet production are small but not negligible at this energy. In our calculation at higher energies[45], we find that multiple jet production has dominant contributions to the high multiplicity events.

3 Jet production in ultra-relativistic nuclear collisions

3.1 Binary collision approximation

In HIJING, a nucleus-nucleus collision is decomposed into binary collisions involving in general excited or wounded nucleons. Wounded nucleons are assumed to be $q-qq$ string-like configurations that decay on a slow time scale compared to the collision time of the nuclei. In the FRITIOF scheme wounded nucleon interactions follow the same excitation law as the original hadrons. In the DPM scheme subsequent collisions essentially differ from the first since they are assumed to involve sea partons instead of valence ones. In HIJING we adopt a hybrid scheme, iterating string-string collisions as in FRITIOF but utilizing DPM-like distributions as in Eqs. 33, 34. Another difference in the way soft interactions are treated in HIJING is that string-string interactions are also allowed to de-excite as well as excite further the strings within the kinematic limits. In contrast, in the FRITIOF model multiple interactions are assumed to lead only to excitations of greater mass strings. Many variations of the algorithm for multiple soft interaction are of course possible as emphasized before. The one implemented in HIJING is simply a minimal model which reproduces essential features of moderate energy pA and AA data.

The binary collision approximation is of course valid for rare hard scatterings. In that case, multiple hard processes involve independent pairs of partons. Only very

rarely does a given parton suffer two high p_T scatterings in one event. As the energy increases the number of partons that can participate in moderate $p_T > p_0$ processes increases rapidly and initial state interactions can lead to nuclear shadowing phenomenon as will be discussed in the next subsection. However, the basic independent binary nature of the multiple mini-jet production rate is expected to remain a good approximation as long as Eq. 6 holds.

The number of binary collisions at a given nuclear impact parameter is determined by Glauber geometry. We employ three-parameter Wood-Saxon nuclear densities determined by electron scattering data[46] to compute that geometry as done in ATTILA[6].

For each binary collision, we use the eikonal formalism as given in Section 2.1 to determine the probability of collision, elastic or inelastic and the number of jets it produces. After a hard scattering, the energy of the scattered partons is subtracted from the nucleon and only the remaining energy is used to process the soft string excitation. The excited string system minus the scattered hard partons suffers further collisions according to the geometric probabilities.

After all binary collisions are processed, the scattered gluons from each nucleon are arranged according to their rapidities and connected to the valence quarks and diquarks of that nucleon in the collision. The rare hard scatterings of q-$\bar{q}$ pairs with opposite flavors are treated as a special case and processed as independent strings.

As we have mentioned before, soft interactions which will accompany almost every nucleon-nucleon collision result in a low transverse momentum transfer to the quarks or diquarks. Multiple inelastic interactions can also effectively increase the initial p_T of partons prior to a hard scattering event. This is a form of initial state interactions that can have some modest effect on hard processes in nuclei. This together with the intrinsic parton p_T already included in PYTHIA leads to an enhanced acoplanarity of jets in nuclear collisions. We assume that the distribution of such initial state

transverse momentum kicks is given by the same distribution as in Eq. 35. The effect of this initial state interaction can be tested in jet production in pA reactions, as will be discussed in another publication.

3.2 Nuclear shadowing effect

At $\sqrt{s} = 200$ (2000) GeV/n, the mini-jet inclusive cross section from Fig. 1 is $\sigma_{jet} \sim 10$ (70) mb. For $Au + Au$ collisions, a central core of area $\sigma_{in} \approx 40$ mb could have up to ~ 50 binary interactions on the average. Assuming additivity of the nuclear structure functions, $f_{a/A}(x, Q^2) = A f_{a/N}(x, q^2)$, the average number of mini-jets produced in that core is then $\sim$ 12 (84). Since the production area of mini-jets is $\sim$ 0.3 mb, the fraction of the transverse area σ_{in} involving mini-jet processes is then 0.1 (0.6)$<$ 1. Thus, up to $\sqrt{s} = 2000$ GeV/n, the multiple mini-jet processes can be treated approximately as independent "hot spots". However, this upper limit is conservative since nuclear shadowing, as we discuss below, reduces the number of mini-jets actually produced.

The number density, $f_{a/A}(x, p_0^2)$, of initial partons (mostly gluons) at the scale $x \sim 2p_0/\sqrt{s}$ is not additive in the nucleon number as $x \to 0$. At small x, nuclear modifications of the parton structure functions are expected. In particular it is known[47] that the number of quarks and antiquarks in a nucleus is depleted in the low region of x. Several mechanisms have been proposed to explain this so-called nuclear shadowing effect based on the parton model. One of them[48] attributes the shadowing effect to the destructive interference which diminishes the flux and interactions of partons in the interior and back face of the nucleus. Another[49] ascribes shadowing to gluon recombination at high densities. While data exists on quark shadowing to constrain and test such models, nothing is known directly on gluon shadowing which is most relevant for multiple mini-jet production.

In HIJING we have included a simple parameterization of gluon shadowing to test

the sensitivity of the final distributions to this aspect of nuclear dynamics. While theoretically there may be differences between quark and gluon shadowing[50], we assume for simplicity that the shadowing effects for gluons and quarks are the same. We also neglect the possible QCD evolution of the shadowing effect, because experiments find no prominent Q dependence of the nuclear effect on quark structure function. At this stage, the experimental data unfortunately cannot fully determine the A dependence of the shadowing even for quarks. We will follow the A dependence proposed in Ref. [49, 51] and use the following parametrization,

$$\begin{aligned} R_A(x) &\equiv \frac{f_{a/A}(x)}{A f_{a/N}(x)} \\ &= 1 + 1.19 \ln^{1/6} A \left[x^3 - 1.5(x_0 + x_L)x^2 + 3x_0 x_L x\right] \\ &\quad - \left[\alpha_A - \frac{1.08(A^{1/3}-1)}{\ln(A+1)}\sqrt{x}\right] e^{-x^2/x_0^2}, \qquad (36) \\ \alpha_A &= 0.1(A^{1/3}-1), \qquad (37) \end{aligned}$$

where $x_0 = 0.1$ and $x_L = 0.7$. The term proportional to α_A in Eq. 36 determines the shadowing for $x < x_0$ with the most important nuclear dependence, while the rest gives the overall nuclear effect on the structure function in $x > x_0$ with a very slow A dependence. As shown in Fig. 14 , this parametrization reproduces the measured overall nuclear effect on the quark structure function in the small and medium x region[47].

Eq. 36 represents only the average nuclear dependence of the structure function. However, in the binary approximation, we have to calculate the effective jet cross section at the nucleon-nucleon level at each impact parameter. Physically, it is natural to expect that the nuclear effects on the structure functions could depend on the local nuclear thickness at each impact parameter[13]. Eq. 37 is consistent with the assumption that the shadowing parameter $\alpha_A(r)$ is proportional to the longitudinal thickness of the nucleus at impact parameter r. We therefore parameterize the impact

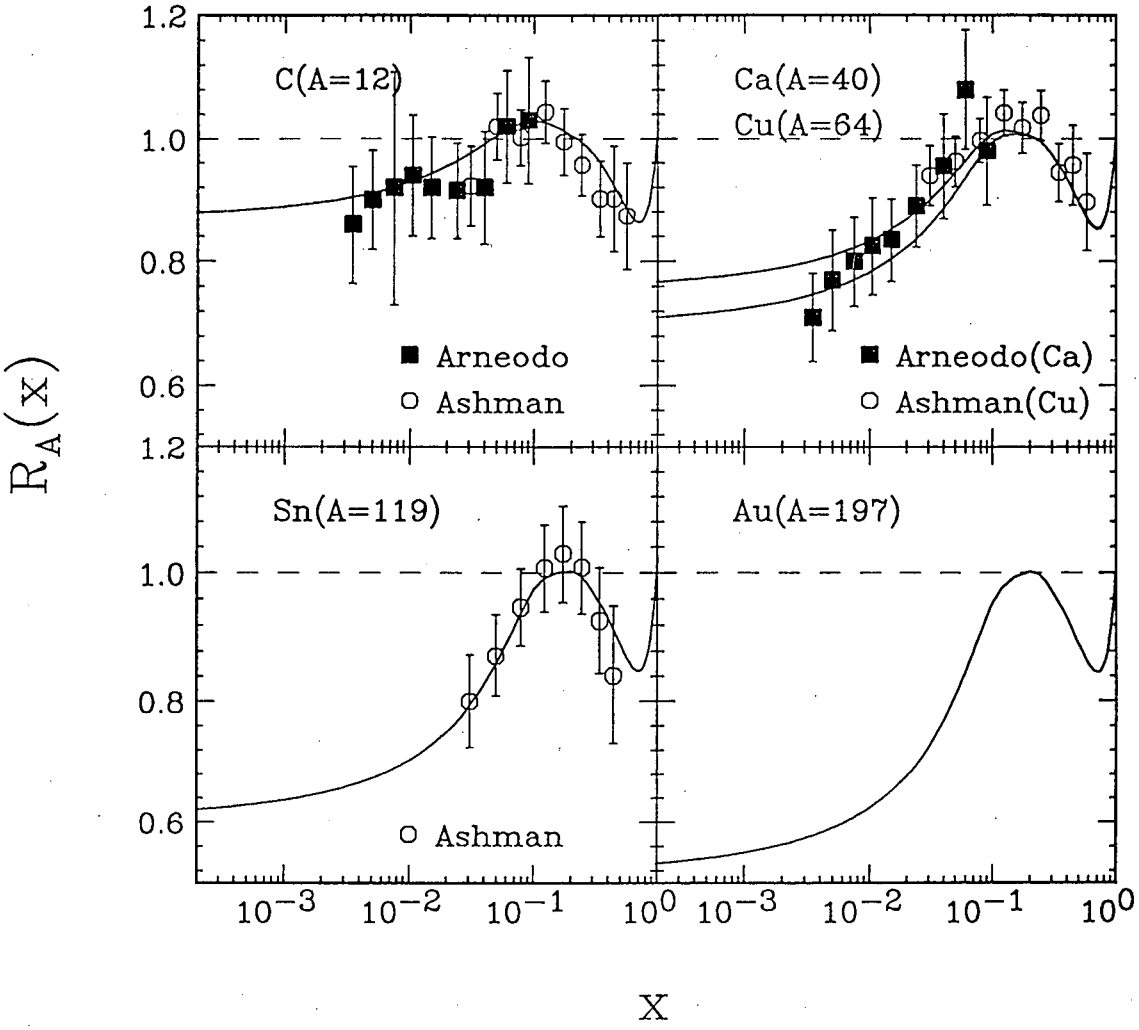

Fig. 14 The ratio of quark structure functions $R_A(x) \equiv F_2^A(x)/AF_2^N(x)$ as a function of x in small and medium x region for different nuclear mass number A. The data are from Ref. [47] and curves are the parametrization in Eqs. 36 and 37.

parameter dependence of α_A in Eq. 36 as

$$\alpha_A(r) = 0.1(A^{1/3} - 1)\frac{4}{3}\sqrt{1 - r^2/R_A^2}, \tag{38}$$

where r is the transverse distance of the interacting nucleon from its nucleus center and R_A is the radius of the nucleus. For a uniform-sphere nucleus with overlap function $T_A(r) = \frac{3A}{2\pi R_A^2}\sqrt{1 - r^2/R_A^2}$, the averaged $\alpha_A(r)$ is $\alpha_A = \int_0^{R_A^2} \pi dr^2 T_A(r)\alpha_A(r)/A$. Because the rest of Eq. 36 has a slower A dependence, we only consider the impact parameter dependence of α_A.

To simplify the calculation during the Monte Carlo simulation, we can decompose $R_A(x, r)$ into two parts,

$$R_A(x, r) \equiv R_A^0(x) - \alpha_A(r)R_A^s(x), \tag{39}$$

where $\alpha_A(r)R_A^s(x)$ is the term proportional to $\alpha_A(r)$ in Eq. 36 with $\alpha_A(r)$ given in Eq. 38 and $R_A^0(x)$ is the rest of $R_A(x, r)$. Both $R_A^0(x)$ and $R_A^s(x)$ are now independent of r. The effective jet production cross section of a binary nucleon-nucleon interaction in $A + B$ nuclear collisions can therefore be decomposed as[13]

$$\sigma_{jet}^{eff}(r_A, r_B) = \sigma_{jet}^0 - \alpha_A(r_A)\sigma_{jet}^A - \alpha_B(r_B)\sigma_{jet}^B + \alpha_A(r_A)\alpha_B(r_B)\sigma_{jet}^{AB}, \tag{40}$$

where σ_{jet}^0, σ_{jet}^A, σ_{jet}^B and σ_{jet}^{AB} can be calculated through Eq. 1 by multiplying $f_a(x_1, p_T^2)f_b(x_2, p_T^2)$ in the integrand with $R_A^0(x_1)R_B^0(x_2)$, $R_A^s(x_1)R_B^0(x_2)$, $R_A^0(x_1)R_B^s(x_2)$ and $R_A^s(x_1)R_B^s(x_2)$ respectively.

In central $Au + Au$ collisions at $\sqrt{s} = 200$ GeV/n, this impact-parameter dependent parton shadowing reduces the averaged inclusive jet cross section with $p_T > p_0$ by 50% from its value in pp. However, at this energy we can see from Fig. 14 that

mini-jet production is still not in the deep-shadowed region of x. For sufficiently high energy, most of the mini-jets come from $x \lesssim 0.01$ region so that the effective mini-jet cross section may be reduced by a factor 3 in central $Au + Au$ collisions. Note that this large reduction of mini-jet multiplicity by gluon shadowing may increase the limit on the independent multi-jet production up to $\sqrt{s} = 50$ TeV/n for $Au+Au$ collisions.

3.3 Jet quenching

Another important nuclear effect on jet production in heavy ion collisions is final state interaction. In high energy heavy ion collisions, hadronic or partonic matter with high density will be produced in the central region. Because this matter extends over a transverse dimension of $\sim R_A$, jets with high p_T will traverse the dense matter for a comparable distance. In Ref. [2] it was suggested that jet quenching resulting from energy loss in that matter may provide a useful probe of the properties of that system. To test this idea more quantitatively we have included an option in HIJING to model jet quenching in terms of a simple gluon splitting mechanism.

The energy loss of a high energy quark or gluon in hot QCD matter has been estimated in Refs. [52, 53, 54]. It appears that radiative energy loss due to induced gluon bremsstrahlung in soft final state scatterings dominates the energy loss mechanism. The radiative energy loss per unit length, dE/dx, in the limit of small mean free path $\lambda_s \ll E/\mu^2$ has been estimated to be[54]

$$dE/dx \approx \frac{3\alpha_s}{\pi}\mu^2 \mathcal{L}(E/\lambda_s\mu^2, s/4\mu^2) \,, \tag{41}$$

where $\mathcal{L}(x,y) = \ln x(\ln x - 1 + 1/x) + \ln y(1 - x/y)$, E is the energy of the propagating parton, $\sqrt{s}$ is the cms energy of the soft interactions and μ is the infrared (Debye) cutoff scale in the matter. In a QGP, $\lambda_s \sim 1/(\alpha_s T)$, $s \approx 6ET$. We note that unlike elastic scattering energy loss[52, 53], the induced radiative energy loss is

perturbatively the same for quarks and gluons[54]. For $\mu = 0.2 - 0.4$ GeV, $\alpha_s = 0.25$ and $T = 0.2$ GeV, a parton with energy of 30 GeV could have an induced radiative energy loss $dE/dx \sim 1 - 2$ GeV/fm. Of course, Eq. 41 only serves as an order of magnitude estimate. It however illustrates that if there is significant variation of $\mu(T)$ near the QGP phase transition at T_c[55], then there could be a significant change of jet quenching as a function of T[54] around T_c.

Induced radiative energy loss is modelled in HIJING by determining first the points of final state interaction of hard partons in the transverse direction and performing a collinear gluon splitting at every point. We assume that interactions only occur with the locally comoving matter in the transverse direction. Interactions with the nuclear fragments is negligible because the two nuclear discs pass each on a very short time scale $2R/\gamma \ll 1$ fm. The interaction points are determined by a probability with a constant mean free path λ_s,

$$dP = \frac{d\ell}{\lambda_s} e^{-\ell/\lambda_s}, \tag{42}$$

where ℓ is the distance the jet has travelled in the transverse direction after its last interaction.

Since the pre-hadronization state in HIJING is represented by connected groups (strings) of valence partons and gluons (kinks), interactions can be easily simulated by transferring a part of the parton energy,

$$\Delta E(\ell) = \ell dE/dx$$

from one string configuration to another. Collinear gluon splitting results in a net jet quenching at the stage of hadronization because the original hard parton energy is shared among several independent strings. This simple mechanism of course conserves

energy and momentum and is numerically simple. A dynamical parton cascade approach (see, *e.g.*, Ref.[56]) involving the space-time development of parton showering is beyond the scope of HIJING.

The main usefulness of our schematic quenching model is to test the sensitivity of the final particle spectra to an assumed dE/dx and λ_s. In particular, one of our motivating goals is to check if the quenching effects produced with $dE/dx \sim 2$ GeV/fm and $\lambda_s \sim 1$ fm can be detected given the large multiple mini-jet background in AA collisions.

3.4 Numerical examples

In this section we apply HIJING to several illustrative problems. Further results emphasizing the novel predictions of this model will be reported elsewhere.

First, to demonstrate that the model works well down to low energies we compare our results in pA and AA collisions with data at SPS energies. We show in Fig. 15 the calculated rapidity distributions of negative charged particles in pp (dot-dashed histogram), pAr (dashed histogram) and pXe (solid histogram) collisions at $E_{lab} =$ 200 GeV. The data are from Ref. [38]. Because jet production is negligible at this energy, the particle production is mainly through soft excitations of projectile and target nucleons. Our low p_T algorithm reproduces the increase of particle production in the central region with the number of participating target nucleons as well as other models[3, 4] in this energy range. The peak of the rapidity is shifted back towards the target region and is proportional to the target atomic number. In the target region, HIJING under-predicts the particle production due to the neglect of final state cascading[10].

Also shown in Figs. 16, 17 are the calculated rapidity distributions of negative particles in central $O + Au$ collisions at $E_{lab} = 60$ and 200 GeV/n, and the transverse momentum distributions of negative particles in $p + p$ and central $O + Au$ collisions at

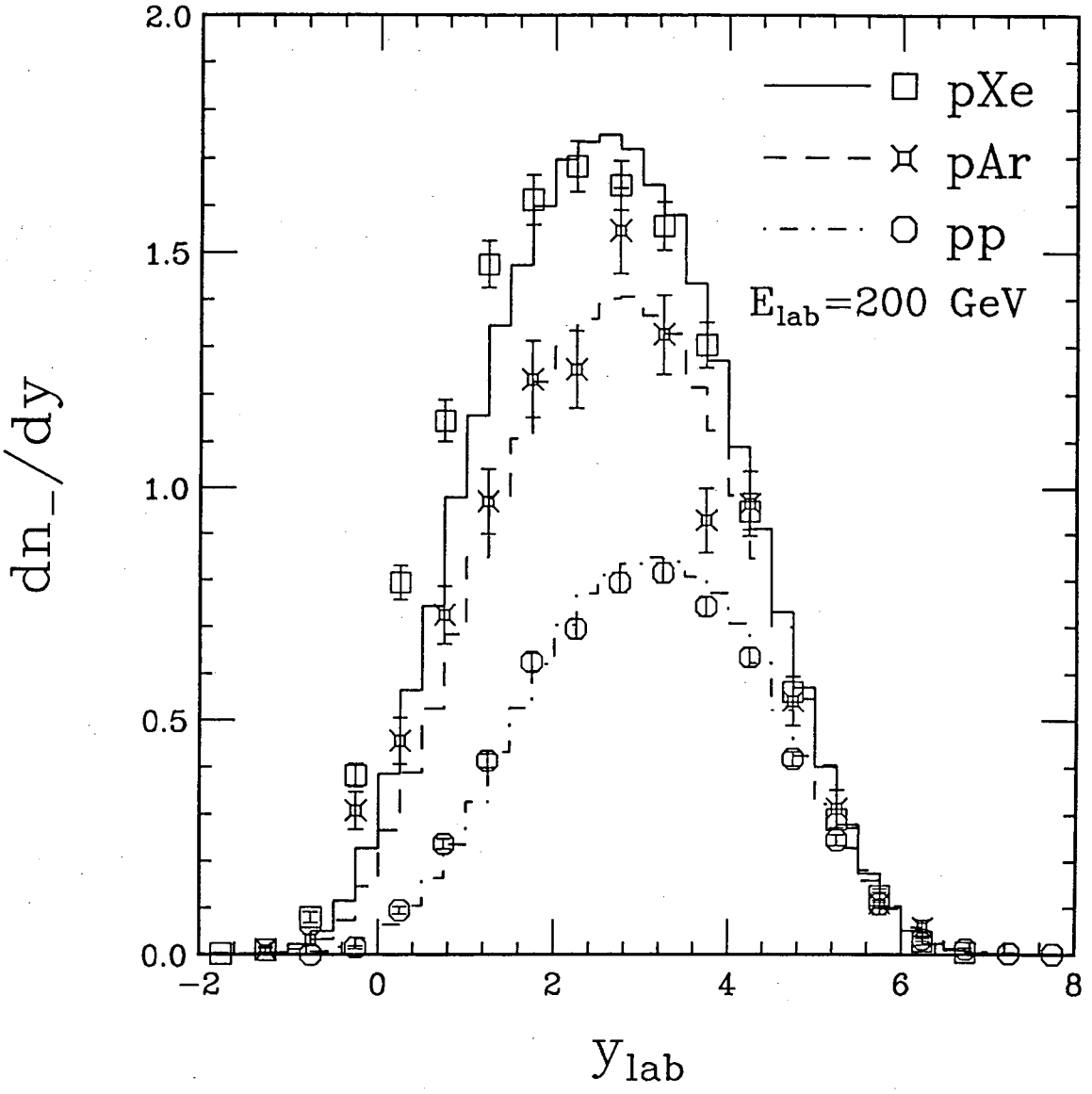

Fig. 15 Rapidity distributions for negative particles in pp (circle, dot-dashed histogram), pAr (crossed-square, dashed histogram and pXe (square, solid histogram) collisions at E_{lab} = 200 GeV. The points are data from Ref. [38] and histograms are from HIJING calculation.

E_{lab} = 200 GeV/n. The overall features of the data[58] are well accounted for except for the enhancement of the low p_T < 0.2 GeV/c in $O + Au$. That enhancement is currently believed to originate also from final state interactions[59]. The data for the $O + Au$ collisions are taken with a central trigger. In our simulations we select central events which can give the corresponding averaged multiplicity. We include these comparisons here only as a necessary test of the multiple soft interaction algorithm in HIJING.

At collider energies, the new physics associated with multiple mini-jet production is expected to lead to new nuclear dependence of multi-particle production. We illustrate this here with the simplest observables: the rapidity and transverse momentum distributions. Shown in Fig. 18, are the calculated pseudo-rapidity distributions of charged particles by HIJING in central (b=0) $Au + Au$ collisions at $\sqrt{s}$ = 200 GeV/n. The solid line is the default result which includes multiple mini-jet production, nuclear shadowing of small x partons and jet quenching. Comparing to the case of only soft interactions (dotted line), jet productions contribute almost half of the total produced particles in the central region.

As can be seen by comparing the curves with and without nuclear shadowing, nuclear shadowing of partons is expected to have a significant effect on particle production at this energy. Without shadowing (dot-dashed line), the particle density in the central region could double our default result. In this calculation the number of pairs of mini-jets produced is reduced from $<N_{jet}>$= 290 to 150 by the parton shadowing. Of course, this number depends sensitively on our assumption that gluon shadowing is the same as quarks and antiquarks. Similar estimates for the magnitude of the shadowing effects was also obtained by Eskola[13]. In that work a smaller effect of shadowing relative to non-shadowing was found for dE_T/dy at this energy because it was assumed that the soft contribution scales as $A^{4/3}$, and thus is substantially larger than in our multi-string model of soft processes.

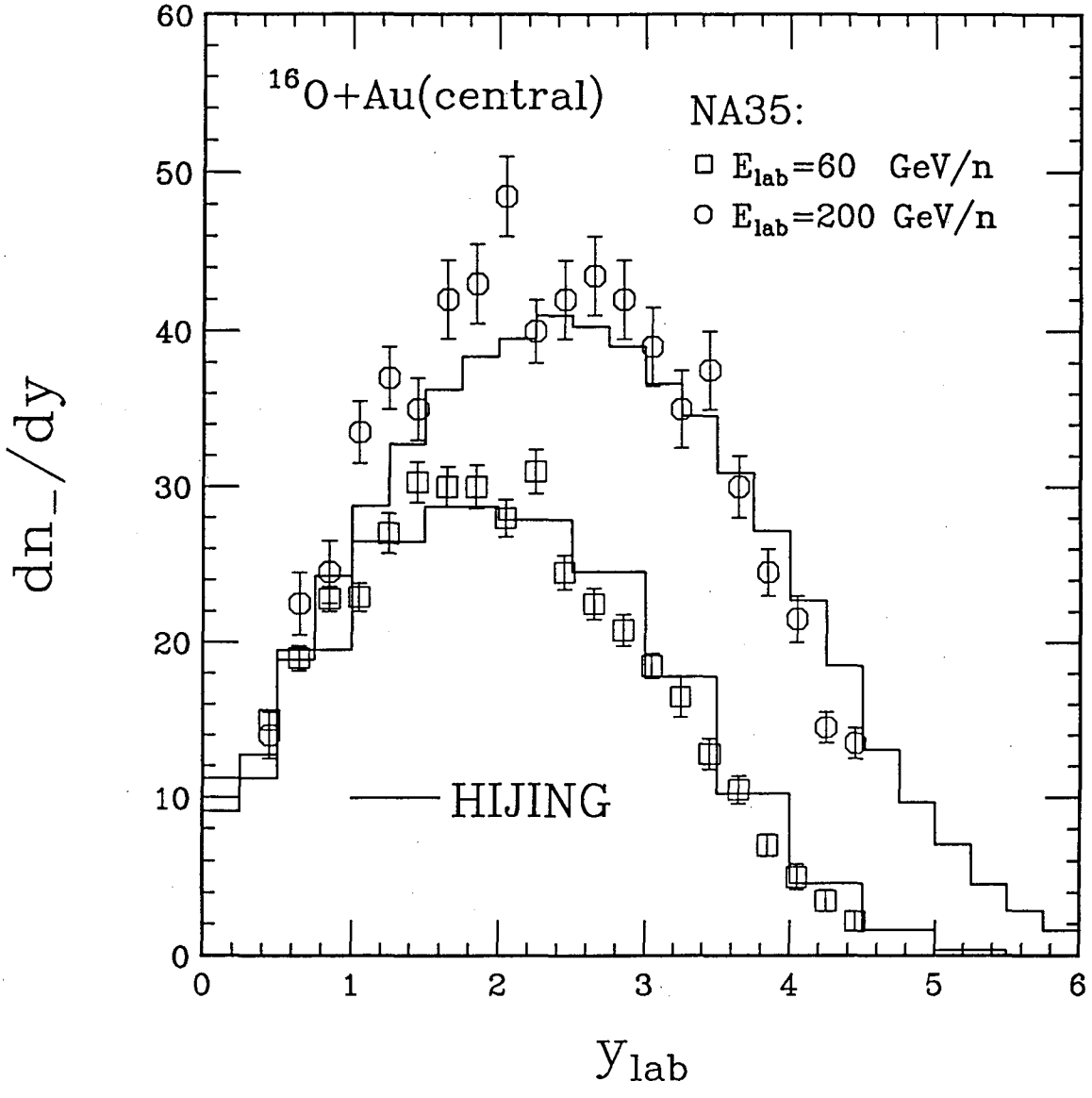

Fig. 16 Rapidity distributions for negative particles in central $O + Au$ collisions at E_{lab} = 60 and 200 GeV/n. The data are from Ref. [58] and histograms are from HIJING calculation.

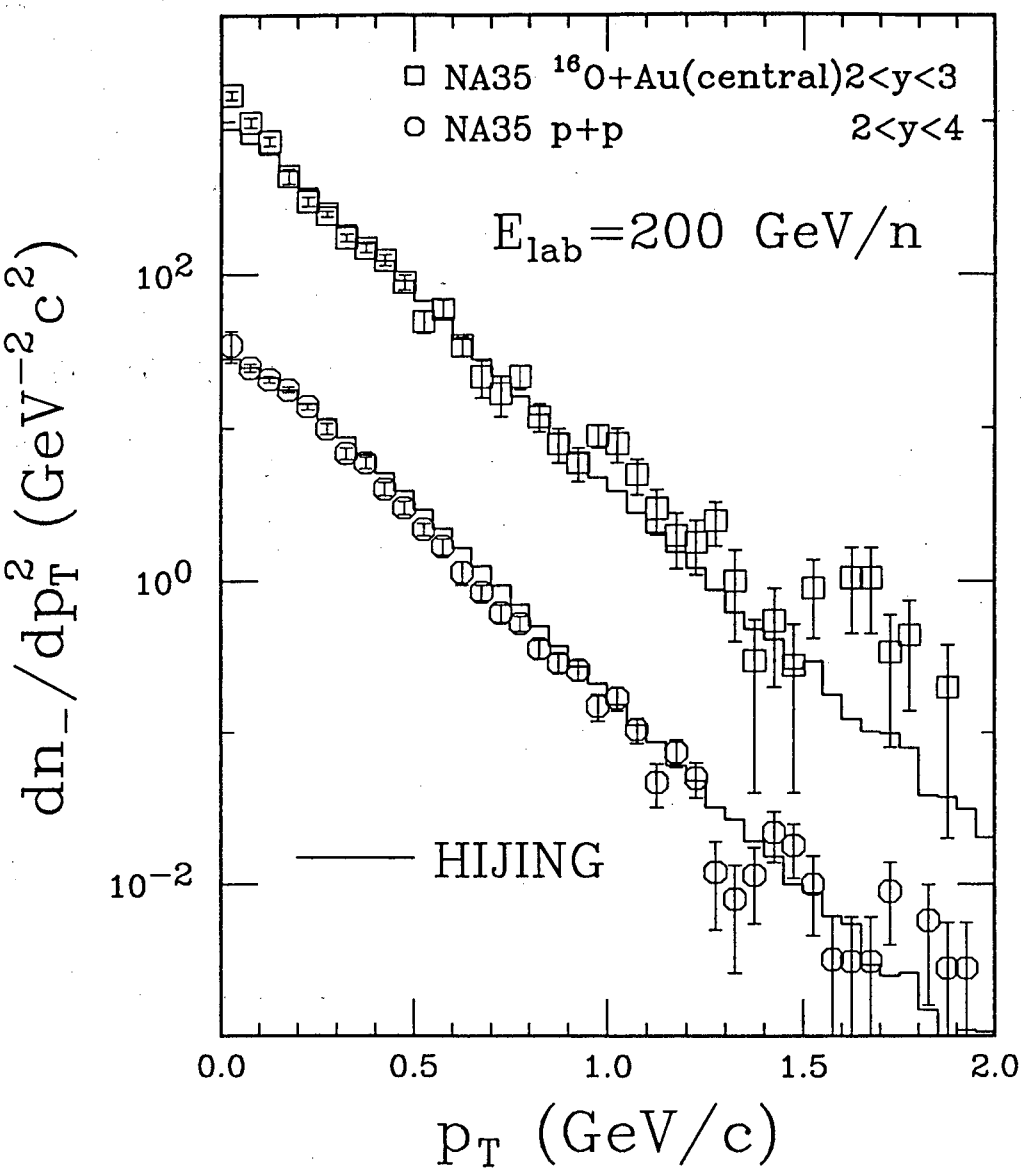

Fig. 17 p_T distributions for negative particles in pp and central $O + Au$ collisions at E_{lab} = 200 GeV/n. The data are from Ref. [58] and histograms are from HIJING calculation.

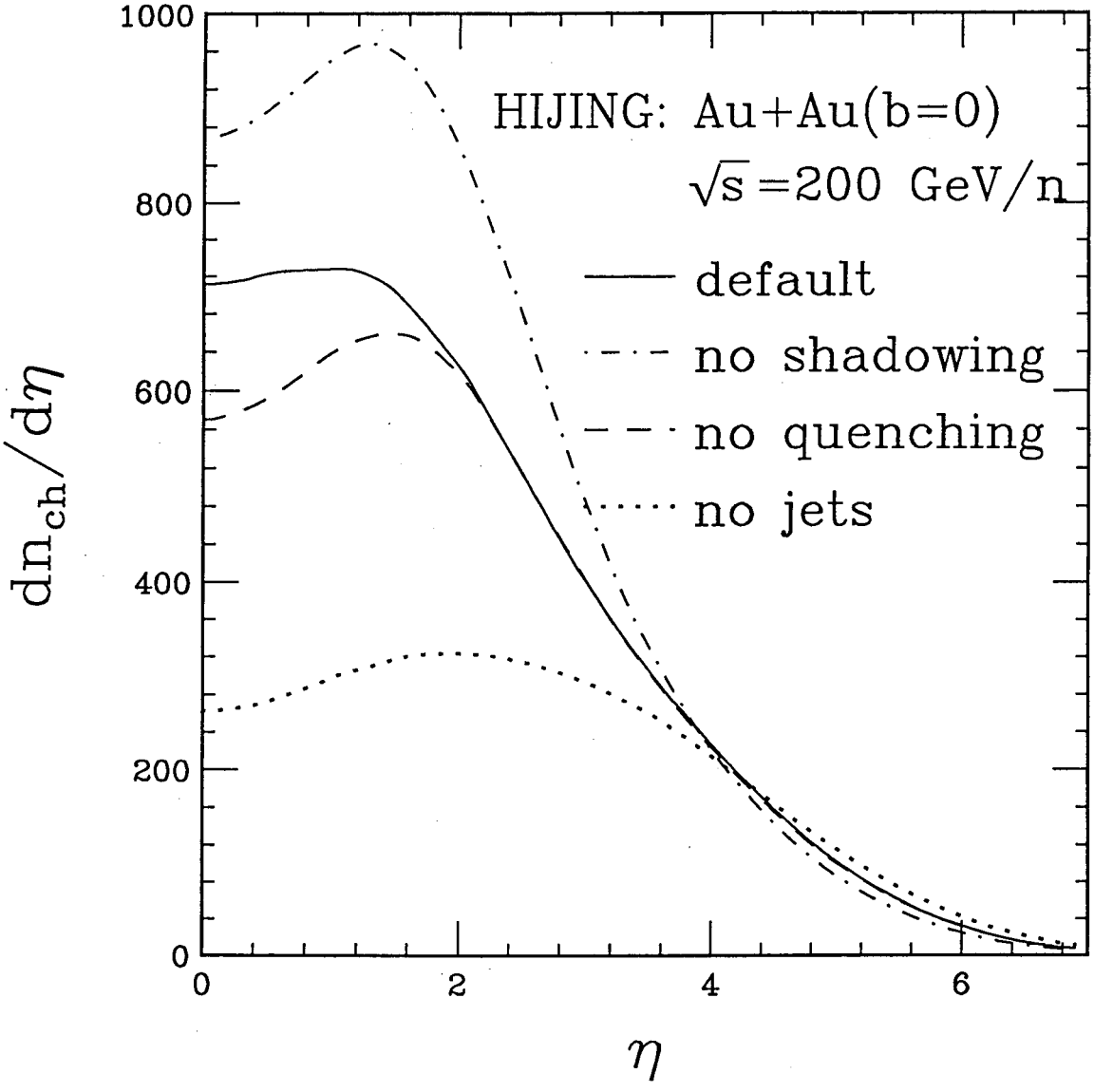

Fig. 18 The prediction of pseudo-rapidity distribution (solid line) by HIJING for charged particles in central $Au + Au$ collisions at $\sqrt{s} = 200$ GeV/n. The dot-dashed line is the prediction without parton shadowing and jet quenching, dashed line is with parton shadowing but without jet quenching and dotted line is without jet production.

At this point it is important to emphasize again the uncertainty associated with the extrapolated soft dynamics from SPS to collider energies. Our extrapolations are conservative in that we assume that the number of beam jets in $A + A$ is simply the number of wounded nucleons,*i.e.*, $2A$. Each wounded nucleon is in turn represented by a string with mass $\propto \sqrt{s}$ and kinks limited to $p_T < p_0$. In DPM-type models[4, 7] additional independent sea $q\bar{q}$ strings are assumed to arise. The number of such strings grows as $A^{4/3}$. However, such low p_T sea strings should be subject to nuclear shadowing just as their moderate $p_T > p_0$ mini-jet counterparts. In addition the assumption of independence of such strings is also questionable because of the absence of a high p_T scale limiting the interaction domain to a small transverse area. Nevertheless, such variations in the soft dynamics cannot be ruled out from first principles and thus must be included in estimating the theoretical uncertainty extrapolating to $A + A$ at collider energies.

In principle, gluon shadowing can be determined via direct photons and jet production in $p + A$, and thus at least the mini-jet contribution could be more reliably determined. The soft contribution, on the other hand, may also be rather sensitive to low p_T final state interactions. Indeed if a QGP is formed in $Au + Au$ collisions then a variety of striking phenomena have been predicted for the low p_T observables. Fig. 18 is therefore only illustrative of the magnitude of expected phenomena.

It is of interest also to compare the result with (solid) and without (dashed line) jet quenching. The quenching mechanism in HIJING is limited to $p_T > 2$ GeV/c partons. This leads to a small enhancement of the low p_T particles in Fig. 18. The effect of jet quenching is of course more pronounced at high p_T. We show in Fig. 19, the p_T distributions of charged particles with $dE/dx = 2$ GeV/fm and $\lambda_s = 1$ fm (solid histogram) and without jet quenching (dashed histogram) in the same central $Au+Au$ collisions at $\sqrt{s} = 200$ GeV/n. We observe a substantial suppression of charged particles at large p_T due to jet quenching in the range of $p_T = 4$ to 8 GeV/c. This effect

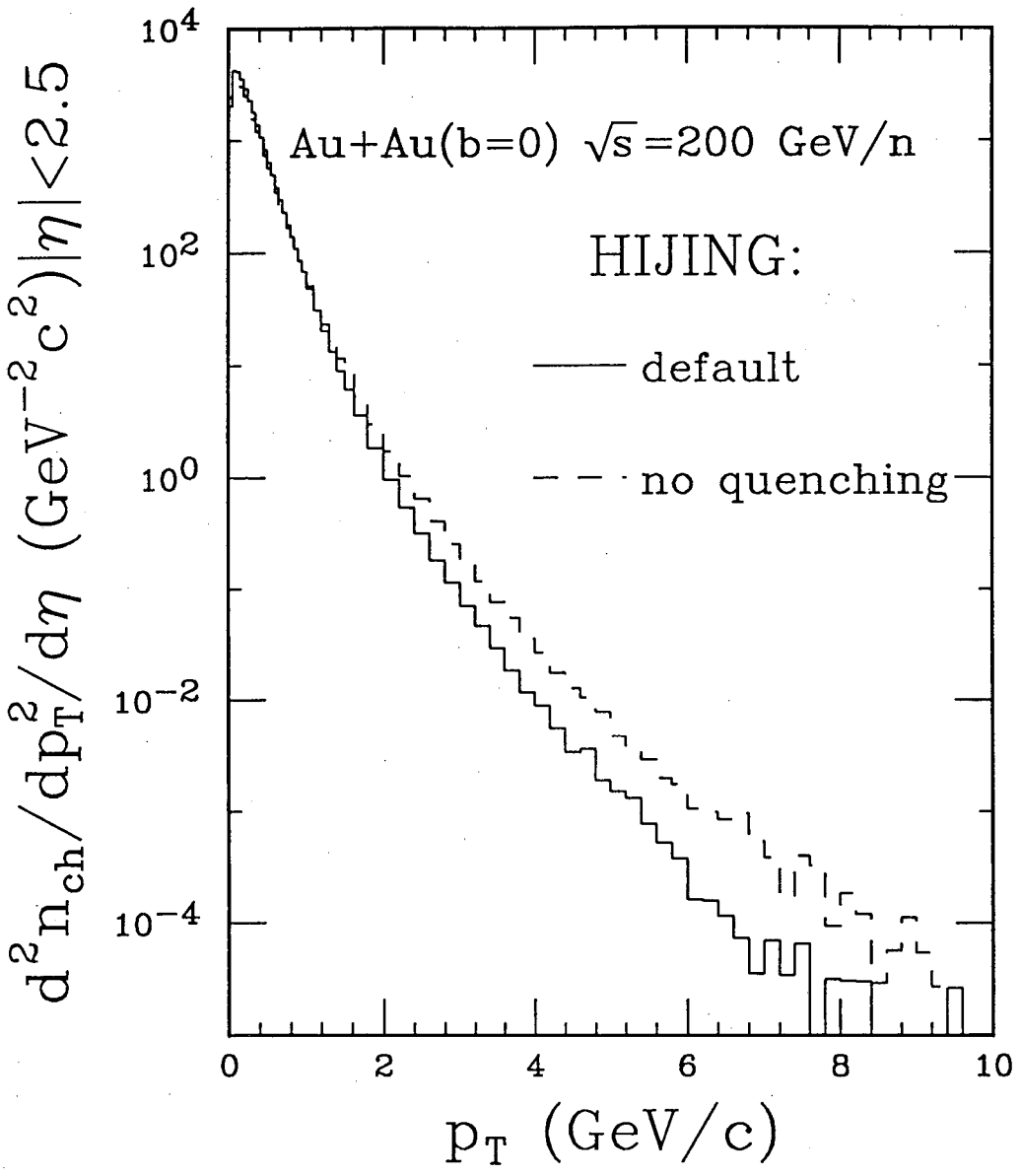

Fig. 19 The prediction of p_T distributions for charged particles by HIJING with (solid histogram) and without (dashed histogram) jet quenching in central $Au + Au$ collisions at $\sqrt{s}$ = 200 GeV/n with $dE/dx = 2$ GeV/fm and $\lambda_s = 1$ fm.

should therefore be easily measurable experimentally. We find that with $dE/dx \sim 2$ there could be a factor of three suppression of high p_T particles in that range. The systematic study of the A dependence of the $p_T \lesssim 10$ GeV/c distributions can thus be used to look for variations in dE/dx as a function of the initial entropy density $\propto dN/dy/R_A^2$ in the search for the QGP transition. This topic will be addressed in more depth in a separate publication.

4 Summary and Outlook

We have developed a new Monte Carlo model, HIJING, to estimate initial conditions via multiple jet production in ultra-relativistic heavy ion collisions. Our starting point was a model for multiple jet production in hadronic interactions in the framework of eikonal formalism and then generalized to the case of $p + A$ and $A + A$ collisions. HIJING provides a consistent framework which is constrained by the available experimental data in low energy $p + A$, $B + A$, and both low and high energy $p + p$ $(p + \bar{p})$ collisions. It also allows the study of novel nuclear effects such as parton shadowing and jet quenching in $B + A$ collisions at collider energies.

Soft interactions leading to beam jets were modelled in the spirit of the FRITIOF and DPM multi-string models with differences as noted. Both excitation and de-excitation of strings is allowed in wounded nucleon-nucleon interactions in a nucleus-nucleus collision. Because we treat explicitly hard QCD processes with $p_T > p_0 = 2$ GeV/c, initial state soft p_T kick and gluon kinks are limited to be below the p_0 scale. We have shown that our low p_T phenomenology accounts for the transverse momentum distribution of produced particles with a consistent Lund string fragmentation scheme. A shortcoming of the present model is the poor agreement with the leading baryon rapidity distributions.

The importance of multiple jet production was confirmed at collider energies for $p + \bar{p}$ collisions. Events with high multiplicity are dominated by multiple mini-jet

production. In particular, they provide a natural explanation for KNO violation at high energies[16]. The increase of the central rapidity density with energy and the development of large p_T tail of inclusive cross sections are also consistently explained with this mechanism. In high energy heavy ion collisions, jets are even more dominating because of the rapid growth of the number of elementary binary collisions. Almost half of the thousands of produced particles in $Au+Au$ can be expected due to mini-jets at $\sqrt{s} = 200$ GeV, even though jet production may be reduced by a factor of two due to the gluon shadowing. Because the particles from hard parton scatterings have a different A dependence from that of soft interactions, the parton shadowing could also influence strongly the nuclear dependence of the central rapidity density in $A + A$ collisions.

We implemented a schematic model for jet quenching with comovers. We found that energy loss of high p_T jets should be easily observed already at the single inclusive level, especially in the moderate $p_T \sim 4-10$ GeV/c range. In a future application we will study the sensitivity of back-to-back di-hadron distributions to this phenomena and whether multi-particle measurements such as calorimetry can be used to extract more information on this dynamical effect. Another important application of HIJING will be the study of jet production in $p+A$ collisions $E_{lab} = 800$ GeV[61]. In particular, an important test of HIJING will be to check whether it can correctly describe the A dependence of the multi-particle background underneath a high p_T jet.

Acknowledgements

We would like to thank B. Andersson, R. C. Hwa, L. McLerran, K. Eskola, J. Carroll, J. W. Harris, P. Jacobs, M. A. Bloomer, and A. Poskanzer for their helpful comments and discussions. We would also like to thank T. Sjöstrand for making available the Monte Carlo program Pythia. We also wish to acknowledge support and fruitful

discussions at the Nuclear Theory Institute at the University of Washington, where part of this work was completed.

References

[1] S. Shuryak, Phys. Rep. **61**, 71 (1980); D. Gross, R. Pisarsky and L. Yaffe, Rev. Mod. Phys. **53**, 43 (1981); H. Satz, Ann. Rev. Nucl. Part. Sci. **35**, 245 (1985); L. McLerran, Rev. Mod. Phys. **58**, 1021 (1986).

[2] M. Gyulassy and M. Plümer, Phys. Lett. **243B**, 432 (1990).

[3] B. Andersson, G. Gustafson and B. Nilsson-Almqvist, Nucl. Phys. **B281**, 289 (1987); B. Nilsson-Almqvist and E. Stenlund, Comp. Phys. Comm. **43**, 387 (1987).

[4] A. Capella, U. Sukhatme and J. Tran Thanh Van, Z. Phys. **C3**, 329 (1980); J. Ranft, Phys. Rev. D **37**, 1842 (1988); Phys. Lett. **188B**, 379 (1987).

[5] T. Sjöstrand and M. van Zijl, Phys. Rev. D **36**, 2019 (1987); T. Sjöstrand, Comp. Phys. Commun. **39**, 347 (1986); T. Sjöstrand and M. Bengtsson, *ibid.* **43**, 367 (1987).

[6] M. Gyulassy, Proceedings of Eighth Balaton Conference on Nuclear Physics, edited by Z. Fodor (KFKI, Budapest, 1987); CERN preprint CERN-TH-4794/87(1987).

[7] K. Werner, Z. Phys. **C42**, 85 (1989).

[8] T. W. Lundlam, BNL Report 51921 (1985); A. Shor and R. S. Longacre, Phys. Lett. **218B**.

[9] J. Aichelin, G. Peilert, A. Bohnet, A. Rosenhauer, H. Stöcker and W. Greiner, Phys. Rev. C **37**, 2451 (1988).

[10] Y. Iga, R. Hamatsu, S. Yamazaki and H. Sumiyoshi, Prog. Theor. Phys. **77**, 376 (1987).

[11] K. Kajantie, P. V. Landshoff and J. Lindfors, Phys. Rev. Lett. **59**, 2517 (1987); K. J. Eskola, K. Kajantie and J. Lindfors, Nucl. Phys. **B323**, 37 (1989).

[12] G. Calucci and D. Treleani, Phys. Rev. D **41**, 3367 (1990).

[13] K. J. Eskola, University of Helsinki preprint, HU-TFT-91-03, 1991.

[14] X. N. Wang and M. Gyulassy, in the proceedings of Fourth Workshop on Experiments and Detectors for a Relativistic Heavy Ion Collider, Upton, New York, July 2-7, 1990, edited by M. Fatyga and B. Moskowitz (BNL-52262,1990), p.79.

[15] A. Capella and J. Tran Thanh Van, Z. Phys. **C23**, 165 (1984); T. K. Gaisser and F. Halzen, Phys. Rev. Lett. **54**, 1754 (1985); P. l'Heureux, *et al.*, Phys. Rev. D **32**, 1681 (1985); G. Pancheri and Y. N. Srivastava, Phys. Lett. **182B**, 199 (1986); L. Durand and H. Pi, Phys. Rev. Lett. **58**, 303 (1987); J. Dias de Deus and J. Kwiecinski, Phys. Lett. **196B**, 537 (1987); R. C. Hwa, Phys. Rev. D **37**, 1830 (1988).

[16] X. N. Wang, Phys. Rev. D **43**, 104 (1991).

[17] X. N. Wang and R. C. Hwa, Phys. Rev. D **39**, 187 (1989).

[18] UA1 Collab., G. Arnison *et al.*, Phys. Lett. **172B**, 461 (1986); and the references therein.

[19] R. D. Field and R. P. Feynman, Nucl. Phys. **B136**, 1 (1978).

[20] B. Andersson, G. Gustafson, G. Ingelman and T. Sjöstrand, Phys. Rep. **97**,31 (1983).

[21] D. W. Duke and J. F. Owens, Phys. Rev. D **30**, 50 (1984).

[22] E. Eichten, I. Hinchliffe,K. Lane and C. Quigg, Rev. Mod. Phys. **56**, 579 (1984).

[23] P. V. Landshoff and J. C. Polkinghorne, Phys. Rev. D **18**, 3344 (1978); C. Goebel, D. M. Scott, and F. Halzen, *ibid.* **22**, 2789 (1980); B. Humpert, Phys. Lett. **131B**, 461 (1983); N. Paver and D. Treleani, *ibid.* **146B**, 252 (1984).

[24] L. Durand and H. Pi, Phys. Rev. D **38**, 78 (1988); T. K. Gaisser and T. Stanev, Phys. Lett. **219B**, 375 (1989).

[25] J. Dias de Deus, Nucl. Phys. **B59**, 231 (1973); **B252**, 369 (1985).

[26] U. Amaldi and K. R. Schubert, Nucl. Phys. **B166**, 301 (1980).

[27] UA4 Collab., M. Bozzo *et al.*, Phys. Lett. **147B**, 392 (1984).

[28] UA5 Collab., G. J. Alner, *et al.*, Z. Phys. **C32**, 153 (1986).

[29] Fermilab E710 Collab., N. Amos *et al.*, Phys. Rev. Lett. **63**, 2784 (1989).

[30] R. M. Baltrusaitis *et al.*, Phys. Rev. Lett. **52**, 1380 (1984).

[31] T. Hara *et al.*, Phys. Rev. Lett. **50**, 2058 (1983). The $p\bar{p}$ cross sections converted from p-air data are taken from L. Durand and H. Pi, Phys. Rev. Lett. **58**, 303 (1987).

[32] UA1 Collab., C. Albajar, *et al.*, Nucl. Phys. **B309**, 405 (1988).

[33] T. Sjöstrand, Comput. Phys. Commun. **27**, 243 (1982).

[34] K. Goulianos, Phys. Rep. **101**, 169 (1983).

[35] J. K. Gunion and G. Bertsch, Phys. Rev. D **25**, 746 (1982).

[36] Bonn-Hamburg-Münche Collab., V. Blobel, *et al.*, Nucl. Phys. **B69**, 454 (1974).

[37] C. Bromberg, *et al.*, Nucl. Phys. **B107**, 82 (1976).

[38] C. De Marzo, *et al.*, Phys. Rev. D **26**, 1019 (1982).

[39] ABCDHW Collab., A. Breakstone, *et al.*, Phys. Rev. D **30**, 528 (1984).

[40] G. Gustafson, Z. Phys. C **15**, 155 (1982).

[41] UA5 Collab., G. J. Alner, *et al.*, Z. Phys. C **33**, 1 (1986).

[42] UA1 Collab., C. Albajar, *et al.*, Nucl. Phys. **B335**, 261 (1990).

[43] British-Scandinavian Collab., B. Alper, *et al.*, Nucl. Phys. **B87**, 19 (1975).

[44] UA5 Collab., R. E. Ansorge, *et al.*, Z. Phys. C **43**, 357 (1989).

[45] X.-N. Wang and M. Gyulassy, to be published.

[46] C. W. Dejager, H. DeVries and C. DeVries, Atomic Data and Nuclear Data Tables, **14**, 479 (1974).

[47] EM Collab., J. Ashman, *et al.*, Phys. Lett. **202B**, 603 (1988); EM Collab., M. Arneodo, *et al.*, Phys. Lett. **211B**, 493 (1988).

[48] S. J. Brodsky and H. J. Lu, Phys. Rev. Lett. **64**, 1342 (1990).

[49] A. H. Mueller and J. Qiu, Nucl. Phys. **B268**, 427 (1986); J. Qiu, Nucl. Phys. **B291**, 746 (1987).

[50] F. E. Close, J. Qiu and R. G. Roberts, Phys. Rev. D **40**, 2820 (1989); A.H. Mueller, CU-TP-441 (1990) preprint.

[51] L. L. Frankfurt and M. I. Strikman, Phys. Rep. **160**, 235 (1988).

[52] J. D. Bjorken, Fermilab preprint Pub-82/59-THY (1982).

[53] M. Thoma and M. Gyulassy, Nucl. Phys. **B351**, 491 (1991).

[54] M. Gyulassy, M. Thoma and X. N. Wang, LBL preprint LBL-31003 (1991).

[55] M. Gao, Phys. Rev. D **41**, 626 (1990).

[56] K. Geiger and B. Müller, Duke University preprint DUK-TH-90-15 (1991).

[57] D. A. Apple, Phys. Rev. D **33**, 717 (1986); J. P. Blaizot and L. D. McLerran, Phys. Rev. D **34**, 2739 (1986); M. Rammerstorfer and U. Heinz, Phys. Rev. D **41**, 306 (1990).

[58] NA35 Collab., H. Ströbele, *et al.*, Z. Phys. **C38**, 89 (1988)

[59] S. Gavin and P. V. Ruuskann, Preprint HU-TFT-90-59.

[60] See papers in the Proceedings of the Seventh International Conference on Ultra-Relativistic Nucleus-Nucleus Collisions, Lenox, Massachusetts, USA, Sept. 26-30, 1988, edited by G. Baym, P. Braun-munzinger and S. Nagamiya, published in Nucl. Phys. **A498** (1989).

[61] Fermilab E557 Collab., C. Stewart, *et al.*, Phys. Rev. D **42**, 1385 (1990).

LAWRENCE BERKELEY LABORATORY
UNIVERSITY OF CALIFORNIA
INFORMATION RESOURCES DEPARTMENT
BERKELEY, CALIFORNIA 94720